ADDIS ABABA UNIVERSITY

ADDIS ABABA INSTITUTE OF TECHNOLOGY

School of Electrical and Computer Engineering

Feasibility Study of Standalone PV/Wind/Biogas Hybrid System for Rural Electrification: (A Case Study of Midrwa Community in Adigrat District)

A thesis Submitted to the Addis Ababa Institute of Technology, School of Graduate Studies, Addis Ababa University

In partial fulfillment of the Requirement for the Degree of

MASTERS OF SCIENCE IN ELECTRICAL ENGINEERING

(ELECTRICAL POWER ENGINEERING)

By

Sisay Fitwi

Advisor: Getachew Bekele (PhD)

August 2014

Addis Ababa, Ethiopia

ADDIS ABABA UNIVERSITY

ADDIS ABABA INSTITUTE OF TECHNOLOGY

School of Electrical and Computer Engineering

Feasibility Study of Standalone PV/Wind/Biogas Hybrid System for Rural Electrification: (A Case Study of Midrwa community in Adigrat District)

BY

SISAY FITWI

GSR/0480/04

APPROVAL BY BORD OF EXAMINERS

______________________	______________________
CHAIRMAN DEPARTMENT OF GRADUATE COMMITTEE	SIGNATURE
Dr.Getachew Bekele	______________________
ADVISOR	SIGNATURE
______________________	______________________
INTERNAL EXAMINER	SIGNATURE
______________________	______________________
EXTERNAL EXAMINER	SIGNATURE

DECLARATION

I, the undersigned, declare that this thesis is my original work, has not been presented for a degree in this or other universities, all sources of materials used for this thesis work have been fully acknowledged.

Name: Sisay Fitwi

Signature: _______________________

Place: Addis Ababa Institute of Technology, Addis Ababa University, Addis Ababa

Date of submission: ____________________

This thesis has been submitted for examination with my approval as a university advisor.

Dr. Getachew Bekele ____________________

Advisor's Name Signature

DEDICATION

...to my beloved mother

Fitsum Haftu

&

My wife

Akberet Tesfay

... *for their incomparable support in all of my academic achievements!*

ACKNOWLEDGMENT

First and foremost, I take this opportunity to give glory to the almighty God, without whom the completion of this work would have been impossible.

Next, I would like to express my sincere gratitude to my advisor, **Dr. Getachew Bekele,** for his expert guidance, constructive comments, suggestions and supports for the successful completion of this paper. He has also played an indispensable role as the primary source of inspiration on every step of the activities or proceedings of my study.

Besides, I would like to acknowledge my families for their continued encouragement in educational and professional pursuits throughout my academic life.

Finally, I need to extend my earnest appreciation to Aksum University for offering me this precious opportunity to pursue my graduate studies. Similarly, I would not pass without extending my heartfelt gratitude to my beloved friends for their valued comments and support during the whole work.

ABSTRACT

So far, Ethiopian Electric Power Corporation utility company uses extension of grids and installation of diesel generators as an option for the electrification of rural villages. Grid expansion to such areas is either financially not viable or practically not feasible as these locations are geographically isolated, sparsely populated and have a very low power demand. The use of diesel generators has also harmful effect on the environment in addition to their higher cost of fuel, maintenance and operation. Consequently, rural areas are dependent on local solutions for electricity supply. These areas have been using Kerosene for lighting, diesel for milling and pumping, traditional biomass as source of energy for cooking and dry cells for radio and tape recorders. However, the current increase in oil price and the negative effects of fossil fuels on the environment motivates to search for other alternative (preferably renewable) sources of energy.

In this work, feasibility of PV-Wind-Biogas hybrid system with battery storage as a backup is studied to electrify the village in Adigrat district. It also compares the cost of the hybrid system against the cost required to electrify the village by extending the grid. The feasibility of this paper is analyzed using HOMER (Hybrid Optimization Model for Electrical Renewable) software. The data for biogas energy potential estimation is obtained from the Ministry of Mines and Energy (MME) of Ethiopia. The paper utilized meteorological data obtained from National Meteorological Agency of Ethiopia, NASA and SWERA to estimate the solar and wind energy potentials. The data needed for calculating the cost of extending the grid is taken from Ethiopian Electric Power Corporation, and is analyzed using interlinked Microsoft office excel spread sheet prepared by Universal Electric Access Program. Electric load estimation and forecasting for the basic needs of the community, such as, for lighting, radio, television, water pumps and flour mills, is done. Primary school and health clinic are also considered for the community. The simulation results show many feasible hybrid system combinations having a cost of energy less than $0.295/kWh which is much lower than diesel generators and previously studied PV/Wind hybrid systems. The hybrid energy system optimized by HOMER for this village is cost effective as compared to the cost required to electrifying the village. The breakeven grid extension distance is found to be 14.9kms, which implies that this hybrid energy system is cost-effective for areas greater than the breakeven distance.

Keywords: national grid, wind energy, photovoltaic, biogas energy, HOMER, PV-wind-biogas hybrid, standalone system, breakeven grid extension distance

TABLE OF CONTENTS

LIST OF FIGURES

LISTS OF TABLES

NOMENCLATURE

a	regression coefficient
A	the diode quality/curve fitting factor
A	the swept area of wind turbine (m^2)
AD	Anaerobic Digestion
b	regression coefficients
B_R	organic load ($kg/d*m^3$)
BTTP	block type thermal power plant
c	A scale parameter of Weibull distribution (m/s)
c	concentration of organic matter(%)
c	the biogas yield per unit dry mass
CC	Cyclic charge dispatch strategy
CFL	Compact fluorescent lamp
CH_4	methane
CHP	combined heat and power
CNG	compressed natural gas
COE	Cost of energy ($/kWh)
C_p	the power coefficient of wind turbines
EEPCo	Ethiopian Electric Power Corporation
f_m	fraction of methane in the biogas
GDP	Gross Domestic Product
G_o	extraterrestrial irradiance at any angle of incidence
G_{on}	extraterrestrial irradiance at normal incidence
G_{SC}	The solar constant =1367 (W/m^2)
H	monthly average daily radiation on horizontal surface (MJ/m2)
HAWT	horizontal axis wind turbine
H_b	heat of combustion per unit volume of biogas
H_m	heat combustion of biogas
H_o	monthly average daily extraterrestrial radiation on a horizontal surface (MJ/m^2)

HOMER	Hybrid Optimization and Modeling of Electrical Renewable
HRT	Hydraulic Retention Time (days)
I	the load current (A)
I_a	armature current (A)
I_D	the diode current (A)
I_L	current produced by the cell (A)
I_{mp}	maximum power current (A)
I_o	reverses saturation current of the diode (A)
I_{sh}	current through the shunt resistance (A)
k	A constant known as shape factor of Weibull distribution
K	Boltzmann's constant
Ka	dissociation parameter
LF	Load follow dispatch strategy
LINGO	Optimization Modeling Software for Linear, Non Linear and Integer Programming
m	mass of substrate fed per time unit(kg/d)
m_o	mass of dry input in the digester
MV	medium voltage
n	monthly average daily number of hours of bright sunshine
N	the maximum possible daily hours of bright sunshine given by equation
NASA	National Aeronautics and Space Administration
NH_3	Ammonia
NMSA	National Metrology Service Agency
NPC	Net present cost
PDF	Probability Density Function of wind distribution
P_{pv}	power output of PV array
PV	Photo Voltaic
P_w	power in the wind (W)
Pw_{out}	output power of wind turbine (W)
q	Charge on an electron

Ra	winding/armature resistance (Ω)
SWERA	Solar and Wind Energy Resource Assessment
T	Temperature
t_L	local solar time in hours
t_r	retention time(days)
UEAP	Universal Electric Access Program
V	instantaneous wind velocity
V	output voltage of PV cell (V)
V	volume of substrate fed per time unit(m^3/d)
V(Z)	wind speed at height of Z m (m/s)
V(z)	Wind velocity at height of Z m above ground (m/s)
$V(Z_{ref})$	wind speed at the reference height (m/s)
VAWT	vertical axis wind turbine
V_b	volume of biogas
v_f	flow rate of the digester fluid
VFA	volatile fatty acid
Voc	open circuit voltage (V)
V_R	digester volume (m^3)
Z	height where wind speed is to be determined (m)
Z_o	Surface Roughness length (m)
Z_{ref}	reference height (m)
$\bar{V}$	mean wind speed (m/s)
α_s	solar altitude (^{0})
γ_s	solar azimuth (^{0})
η_t	Overall efficiency of the transmission system/power train of wind turbine
η_t	the efficiency of power conditioning equipment (≈90%)
θ_i	the angle between the solar beam and normal to the solar panel
θ_z	zenith angle (^{0})
ρ_m	density of the dry matter in the digester
ω_s	The sunset hour angle

δ	declination angle(^{0})
η	combustion efficiency of burners(boilers)
ρ	density of air
ω	solar hour angle (^{0})
ϕ	latitude(^{0})

CHAPTER ONE

INTRODUCTION

1.1. Background and Statement of the Problem

Ethiopia with landmass of 1.1million square kilometers is the third giant and second populous nation in the Sub-Saharan Africa with estimated population of about 85.5million [1]. According to the UNDP by 2010, Ethiopia ranked 157th out of 169 countries in the human development index, with per capita average annual income of 120$ and about 40% of the population below poverty line [1]. As 2009/2010 report from Ethiopian Electric Power Corporation (EEPCo) figure indicate, 85% of the population lives in rural areas and the electricity access by the country has reached 41% from 15%. However, most of the customers live in urban areas and consume less than 50 kWh per year, while rural area electricity coverage is almost negligible (less than 2%) [2, 3].

EEPCo has a short and long term plan to increase the existing generation capacity to fill the gap. The 2 GW generation capacity will be increased to 10 GW in the coming five-six years. This is mainly achieved by constructing new hydropower plants including the Grand Ethiopian Renaissance dam with a capacity of 6000 MW. Although there is high potential in hydro power, vast use of the resource is not implemented. This is due to the fact that the service giving dams are being affected by climate change and hydrological problems. Additionally, the installation and erection of hydropower system takes long time. Hence, due attention should be given to development and diversification of the power system with renewable energy sources which are cost effective in reaching the remote areas. It is also necessary to increase the current power generation mix; to cover increasing power demand and avoid dependence on fuel imports.

UEAP under EEPCo has planned to electrify majority of the rural community. However, due to capacity constraints and difficult geographical layout of the remote locations, grid connection of remote villages has not been possible. Consequently, rural areas are dependent on local solutions for electricity supply. These areas have been using Kerosene for lighting, diesel for milling and pumping, traditional biomass as source of energy for cooking and dry cells for radio and tape recorders. However, the global price increase of oil and negative effects it imposes on environment has enforced to search for other energy alternatives.

The rural areas of Midrwa are among the villages of Ethiopia facing similar problems due to the difficulty of giving electric access by extending the grid. This can be minimized by looking for alternative resources which can be used as a stand-alone to give electric access to the community. The thesis proposes hybrid of solar, wind and biogas available energies as a first option for electrification. Figure 1.1 shows the living style of individuals in the village. The village is located 30kms far from Adigrat town, Fig 1.2.

Figure 1.1: Living style of rural area communities

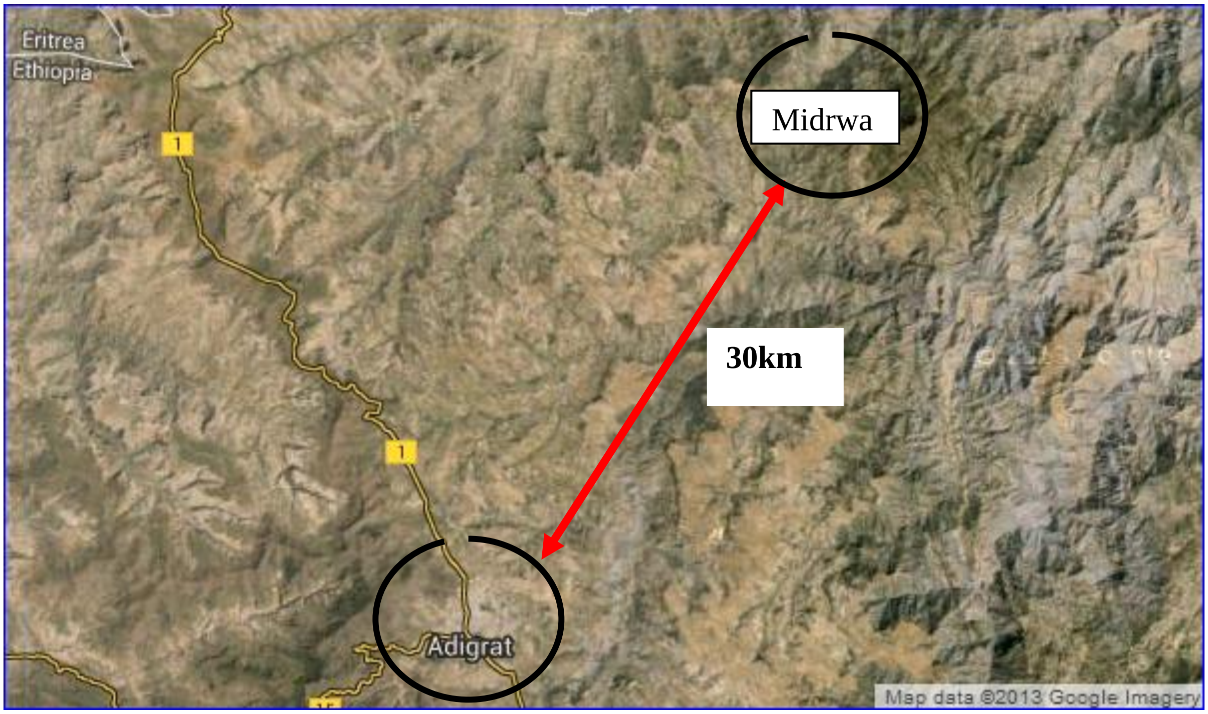

Figure 1.2: Google map picture of study area distance from Adigrat town

1.2. Objectives of the Study

The main objective of this thesis is to study the feasibility of solar photovoltaic, wind and biogas energy system for hybrid electrification of remote villages in Adigrat district.

Specific Objectives

To achieve the main goals, the study has the following specific objective:

- To study the solar photovoltaic, wind and biogas energy potential of the study area.
- To estimate and forecast the energy demand of the Midrwa village areas by considering the basic needs of the people.
- To select appropriate solar modules, wind turbines, biogas generator and batteries depending on the energy demand.
- To model hybrid renewable energy system for the community in Midrwa, and
- To compare the investment cost of the hybrid system against the cost required to electrify the areas by extending the national grid.

1.3. Methodology

Site Identification

The selected off-grid remote rural village for this thesis is Midrwa. It is a small village in the Adigrat district in the Tigray region of Ethiopia. Figure 1.2 above shows the location of the village on the map. It is located at 14°00' N and 39°27' E and has an average elevation of 1731 meters.

Data Collection and Feasibility Study

As it is mentioned in the introduction section, this research is mainly concerned to looking in- to better option of energy sources to electrify villages in remote areas of Ethiopia which are isolated from the national grid by comparing against the cost needed to extend the national grid. The main concern is the assessment of resource potential and modeling of the hybrid system by analyzing the data taken from different sources.

The field data which includes the number of households and their daily activities related to energy consumption is collected by visiting the selected village. However, wind speed and solar radiation of the sites collected from NASA and SWERA is compared with the data's from NMSA of Ethiopia. The data required for biogas which is the cattle's manure is collected from Ministry of Mines and Energy. The data needed for calculating the cost of extending the grid is taken from EEPCo, and is analyzed using interlinked Microsoft office excel spread sheet prepared by UEAP. Finally the hybrid system is modeled and simulated using HOMER software based on the data collected to get the best optimization.

1.4. Related Works

Drake F. and Mulugeta Y. [4, 5] studied the solar and wind potential distribution of Ethiopia. Regression coefficients of the angstrom equation (a and b) relating sunshine duration to daily solar radiation and Weibull parameters (shape factor, K, and the scale factor, c) are estimated throughout the country. Bekele G. [6, 7] determined solar and wind potentials of selected locations in Ethiopia and studied feasibility of Wind/PV hybrid system to electrify 200 model families using HOMER for optimization and sensitivity analysis. Tamirat B. [8] has made a feasibility comparison of independent electrification at Dillamo and Gode sites in Ethiopia by either of the wind, solar PV or micro hydropower system. But, the author didn't consider the possibility of combining the resources into hybrid system and the analysis is done manually without any computer tool.

Janani Chakravarthi[9] presented a paper of biogas and energy production biogas can be produced from a number of sources such as municipal waste, corn husk, farmland manure, to name a few. Treating animal waste with the technology of an aerobic digestion can reduce environmental pollution and generate relatively cheap and readily available source of energy in diary farms. The gas produced can be used for space and water heating of farm house, for cooking, lighting, grain drying and as fuel for heating greenhouses during cold weather. Stages, new integrated approaches and economic considerations were briefly discussed. [10] J. K. Maherchandani, Chitranjan Agarwal, Mukesh Sahi used Homer software for his simulation and it emphasizes the use of renewable hybrid power system to obtain a reliable autonomous system with the optimization of the components size and the improvement of the capital cost. The main source of power to the energy system is biomass generator, whereas, photovoltaic panels and wind generators are the supported additional sources. The results showed as biomass generator is chosen as a major source of power in the rural areas due to its high efficiency and cost effectiveness. [11] Studied off-grid electrification of seven villages in the Almora district of Uttarakhand state, India. In their study, biomass, solar, hydro and wind energy sources were considered and analyzed using LINGO and HOMER software. [12] The study of PV-Wind-Hybrid systems for stand-alone applications on Swedish locations has been performed with the simulation tool HOMER. Its aim was to evaluate the system costs, the cost of energy generated by the PV-Wind- Hybrid systems, the effect of the load size and to what extent the combination of these two energy sources can reduce the costs compared to a PV-alone system. This simulation resulted in reduction of NPC, and showed stand-alone hybrid system applications have the potential to be more efficient compared to PV alone system.

The main focus of this thesis work is to assess the solar, wind and biogas power potentials of Midrwa community found at Adigrat district. It also compares the hybrid system against the investment cost required to electrify the village using grid extension. At the end, it proposes optimal hybrid combinations for rural electrification of 200 model community using HOMER as optimization and simulation tool.

1.5. Organization of the Thesis

This thesis is organized into six chapters. The first chapter is about the background of the study and statement of the problem, objective, methodology and related works to this thesis. The second chapter presents the basic theory of solar PV system and the potential at Adigrat district. The third and fourth chapter discusses the basic theories of wind and biogas systems together with their potential estimations at Adigrat district respectively. The fifth chapter presents the application of HOMER for PV-wind-biogas hybrid system and cost analysis of grid extension. At last, the sixth chapter brings to an end of this research with results of the thesis, conclusions and recommendations.

CHAPTER TWO

SOLAR ENERGY SYSTEMS AND SOLAR ENERGY RESOURCES

2.1. Introduction

The sun is the largest energy source of life at the same time it is the ultimate source of all energy (except tidal and geothermal power), even the energy in the fossil fuels ultimately comes from the sun. The sun radiates 174 trillion kWh of energy to the earth per hour. In other words, the earth receives 1.74 x 10^{17} watts of power from the sun [13].

The sun is a typical star with mass 2×10^{30} kg, beam length 700,000 km and it has roughly 5 billion more years of life. Its surface temperature is about 5800 Kelvin while the internal temperature is approximately 15 million Kelvin. This temperature derives from reactions which were based on the transformation of hydrogen to helium, the process called nuclear fusion, which produces high temperature of the sun and the continuous emission of large amounts of energy. It is calculated that for each gram of hydrogen that is converted to helium sun radiates energy equal to 1.67×10^{5} kWh. The solar energy is emitted to the universe mainly by electromagnetic radiation. Approximately one-third of energy radiated from sun is reflected back. The rest is absorbed and retransmitted to the space while the earth reradiates just as energy as it receives and creates a stable energy balance at a temperature suitable for life.

2.2. Solar Photovoltaic Energy

Photovoltaic (PV) is a method of generating electrical power by converting solar radiation into direct current electricity using semiconductors that exhibit the photovoltaic effect. PV power generation uses solar panels comprising a number of cells containing a semi-conducting material. As long as light is shining on the solar cell, it generates electrical power. When the light stops, the electricity stops. Many PV have been in continuous outdoor operation on Earth or space for over 30 yrs. [14].

The solar cells that are used on calculators and satellites are photovoltaic cells or modules. This PV module consists of many PV cells wired in parallel order to increase current and in series to produce a higher voltage. When we speak of a PV panel it means any number of PV modules and when we speak of array it means any number of PV panels. Individual PV cells are typically only a few inches in diameter, but multiple cells can be connected to one another in modules, modules can be connected in arrays, and arrays can be connected in very large systems. See Figure 2.1.

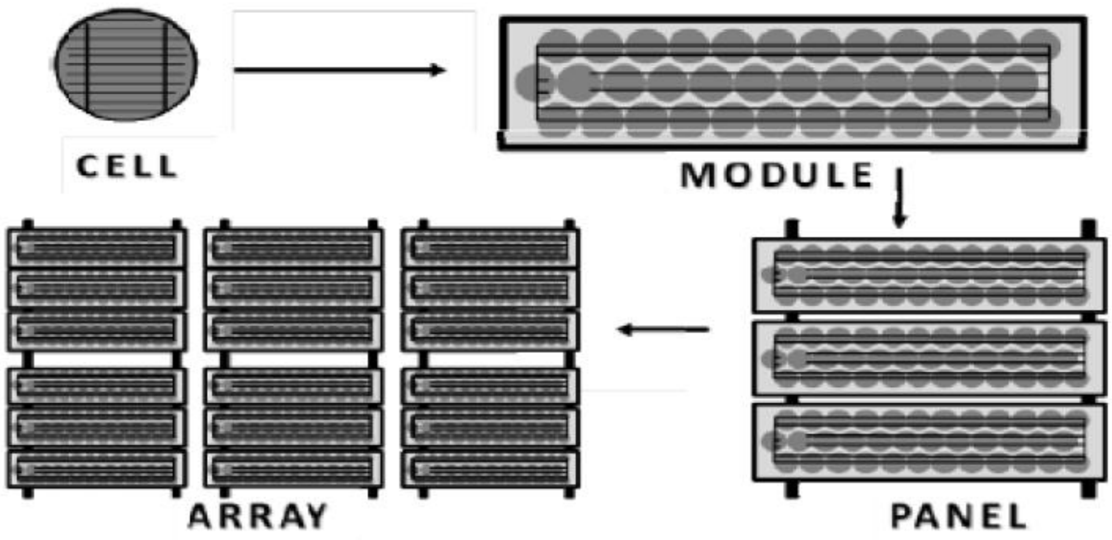

Figure 2.1: PV Diagram [15]

PV panel convert sunlight to DC electricity. The PV generated electricity is 'silent', low in maintenance and does not need in fuel or oil supplies. However, PV energy is available when enough irradiance is accessible.

2.3. General Working Principles Photovoltaic Cells

PV cells convert sunlight directly into electricity by taking advantage of the photoelectric effect. Cells are constructed from semiconductor materials coated with light-absorbing materials. When photons in sunlight strike the top layer of a PV cell, they provide sufficient energy to knock electrons through the semiconductor to the bottom layer, causing a separation of electric charges on the top and bottom of the solar cell. Connecting the bottom layer to the top with a conductor completes an electrical circuit and allows the electrons to flow back to the top, creating an electric current and enabling the cycle to repeat with more sunlight (Clean Energy Associates). Figure 2.2 illustrates how photovoltaic cells work.

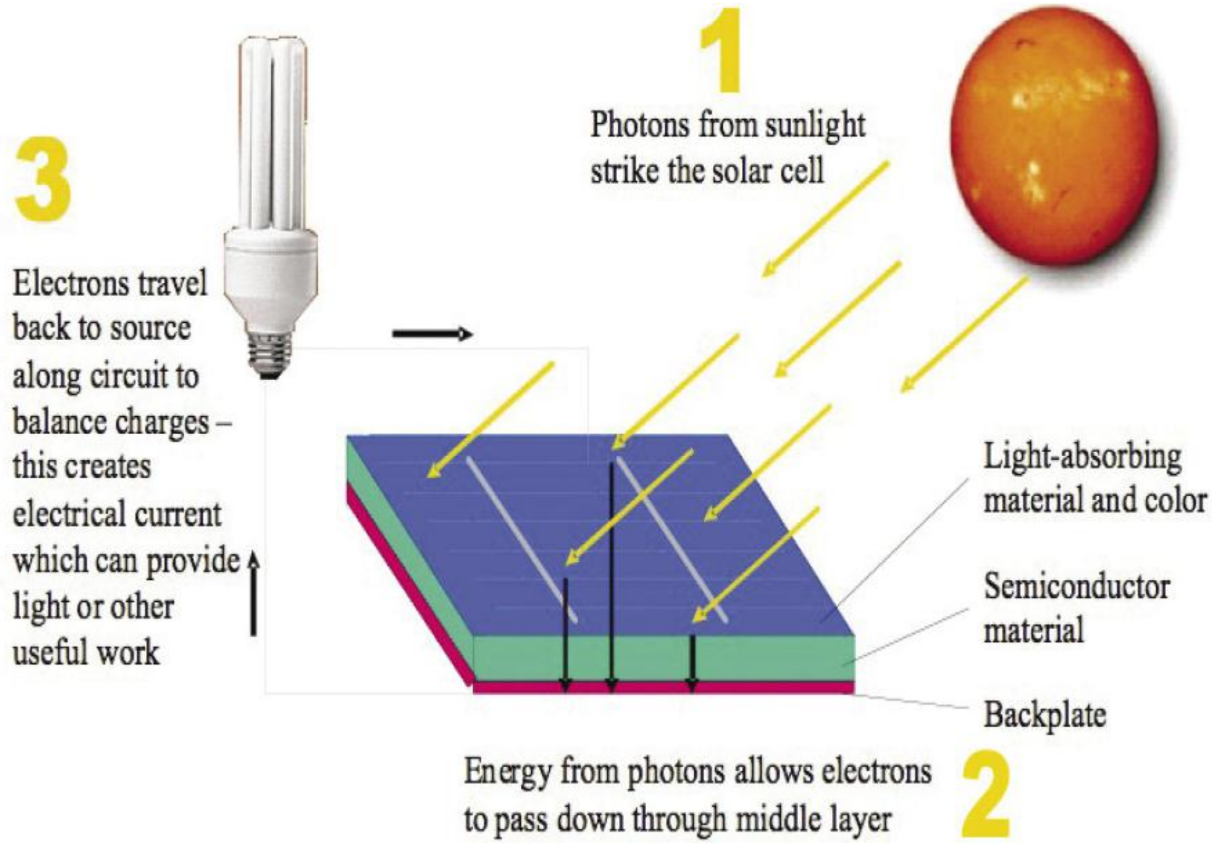

Figure 2.2: How Photovoltaic Cells Work [15]

2.4. Main PV Cell Types

The material that is used widely in the industry for the production of photovoltaic cells is silicon. Based on the structure of the basic material from which they are made and the particular way of their preparation the photovoltaic cells of silicon are categorized into the following four types.

- ***Single-Crystalline Silicon***: The basic material is mono-crystalline silicon. In order to make them, silicon is purified, melted, and crystallized into ingots. The ingots are sliced into thin wafers to make individual cells. It is the oldest and more expensive production technique, but it's also the most efficient and widely used sunlight conversion technology available. Cells efficiency oscillates between 14% and 18% [16].
- ***Polycrystalline or Multi-crystalline Silicon:*** The particular cell is relatively large in size and it can be easily formed into square shape which virtually eliminates any inactive area between cells. It has a slightly lower conversion efficiency compared to single crystalline

and manufacturing costs are also lower. Cells efficiency oscillates between10% and 13% [14].

- ***String Ribbon:*** This is a refinement of polycrystalline silicon production. There is less work in its production so costs are even lower. Cells efficiency averages 8% to 10%**.**
- ***Technology which uses thin film solar cells*** while the total thickness of a semiconductor is about 1μm. Amorphous or thin film silicon cells are solids in which the silicon atoms are much less ordered than in a crystalline form. By using multiple junctions this kind of photovoltaic cells achieve maximum efficiency which is estimated at about 13% while the installation cost is reduced. The efficiency of this cell oscillates between 6% and 10% [15]. Furthermore the output of an amorphous silicon cell is not decreased as temperature increases and is much cheaper to produce than crystalline silicon.

Cells efficiency decreases with increases in temperature. Crystalline cells are more sensitive to heat than thin films cells. The output of a crystalline cell decreases approximately 0.5% with every increase of one degree Celsius in cell temperature. For this reason modules should be kept as cool as possible, and in very hot condition amorphous silicon cells may be preferred because their output decreases by approximately 0.2% per degree Celsius increase [14, 16].

2.5. PV Module and Array

The solar cell is the basic building block of the PV power system. However, it rarely used individually because it is not able to supply an electronic device with enough voltage and power. For this reason, many photovoltaic cells are connected in parallel or in series in order to achieve as higher voltage and power output as possible. Cells connected in series increases the voltage output while cells connected in parallel increases the current. The solar array or panel is a group of several modules electrically connected in series-parallel combination to generate the required current and voltage and hence the power.

A typical photovoltaic system is made of 36 individual 100cm^2 silicon photovoltaic cells and auxiliary devices which are lead-acid batteries with a typical voltage of 12 V. This system has the capacity of producing more than 13V during cloudy days and can charge a 12 V battery.

2.6. Equivalent Electrical Circuit of PV Cell

The complex physics of the PV cell can be represented by the equivalent electrical circuit shown in Figure 2.3 below. The following parameters call for consideration. The current *I* at the output terminals is equal to the light-generated current I_L, less the diode current I_D and the shunt leakage current I_{sh} **.** The series resistance Rs represents the internal resistance to the current flow, and depends on the p-n junction depth, impurities, and contact resistance. The shunt resistance R_{sh} is inversely related to the leakage current to the ground. In an ideal PV cell $R_s = 0$ and $R_{sh} = \infty$. The PV conversion efficiency is sensitive to small variations in Rs, but insensitive to variations in R_{Sh}. A small increase in R_s can decrease the PV output significantly.

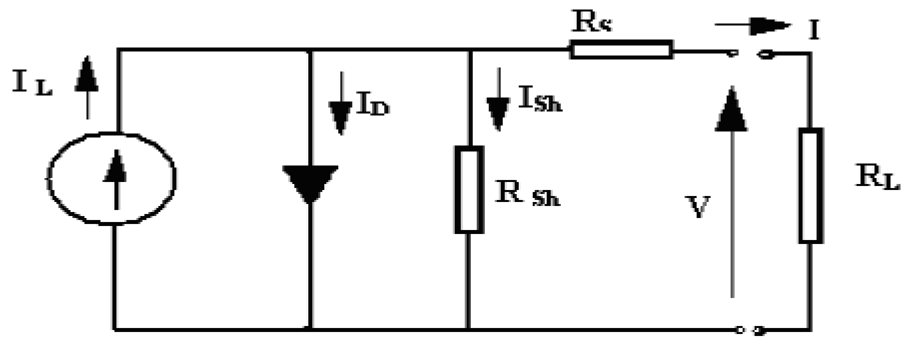

Figure 2.3: A PV cell equivalent electrical circuit [17]

The open-circuit voltage V_{oc} of the cell is obtained when the load current is zero and is given by the following:

$$V_{oc} = (I_L - I_D)R_{sh} \tag{2.1}$$

The diode current is given by the classical diode current expression:

$$I_D = I_o\left[exp\left(\frac{qV_{oc}}{AKT}\right) - 1\right] \tag{2.2}$$

where I_O is the saturation current of the diode (A), q is electron charge (1.6×10^{-19} C), A is curve-fitting constant, K is Boltzmann constant (1.38×10^{-23} J/°K), T is temperature on absolute scale °K.

Thus, the load current is given by the expression:

$I=I_L-I_D-I_{sh}$

$$I = I_L - I_o \left[exp\left(\frac{qV_{oc}}{AKT}\right) - \frac{V_{oc}}{R_{sh}} \right] \tag{2.3}$$

The last term is the leakage current to the ground. In practical cells, it is negligible compared to I_L and I_O and is generally ignored.

The two most important figure of merits widely used for describing PV cell electrical performance are the open-circuit voltage V_{oc} and the short-circuit current I_{sc} under full illumination. The short-circuit current is measured by shorting the output terminals and measuring the terminal current. Ignoring the small diode and ground leakage currents under zero voltage, the short-circuit current under this condition is the photocurrent I_L .

The maximum photo voltage is produced under the open-circuit voltage. Again by ignoring the ground leakage current, equation 2.4 with *I* give the open-circuit voltage as follows:

$$V_{oc} = \frac{AKT}{q} ln\left(\frac{I_L}{I_o} + 1\right) \tag{2.4}$$

2.7. I-V and P-V Curves

The electrical characteristic of the PV cell is generally represented by the current vs voltage (IV) curve. The figure below (Figure 2.4) depicts the I-V curve of typical PV cell. This curve shows the variation of current and voltage when cell resistance varies from zero to infinity. In this curve the point at which the voltage is zero is called the short-circuit current. This is the current we would measure with output terminal shorted. On the other hand the point at which current is zero is known as open-circuit voltage. This is the voltage we would measure with output terminal open. Somewhere in the middle of the two regions, the curve has a knee point.

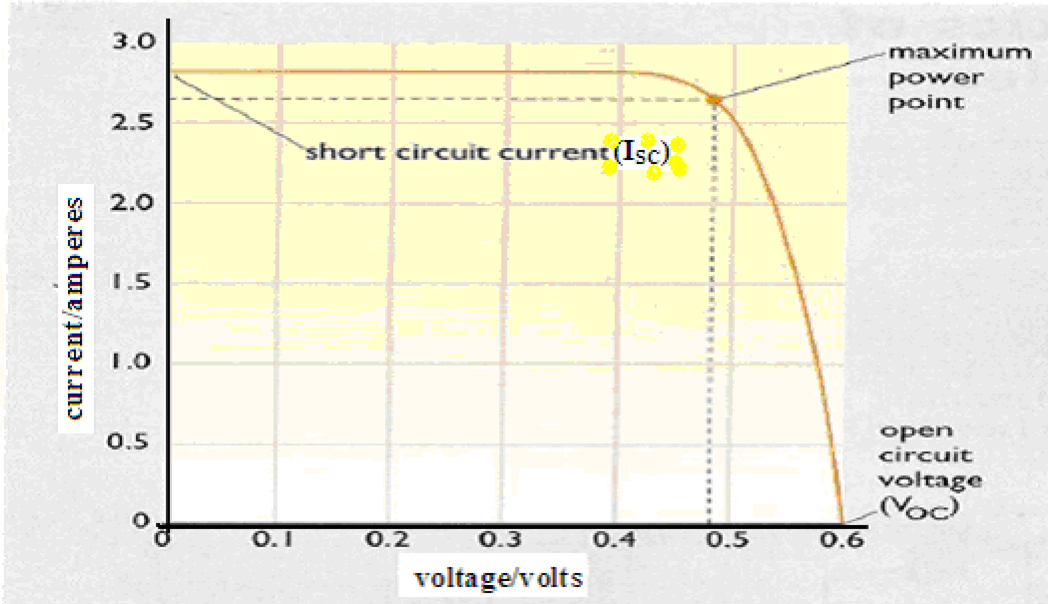

Figure 2.4: I-V Curve of a typical silicon PV [18]

The power output of the panel is the product of the voltage and current outputs. In Figure 2.5, the power is plotted against the voltage which is P-V curve of the PV cell. Note that the cell produces no power at zero voltage or zero current, and produces the maximum power at the voltage corresponding to the knee point of the I-V curve. This is why the PV power circuit is always designed to operate close to the knee point with a slight slant on the left-hand side. The PV circuit is modeled approximately as a constant current source in the electrical analysis of the system.

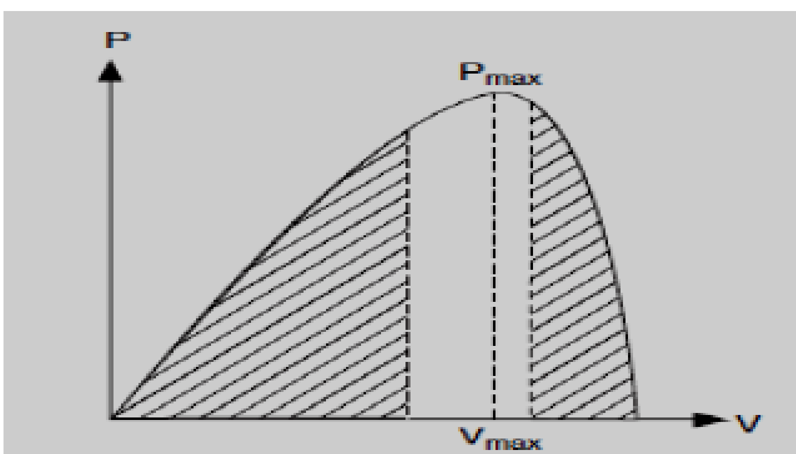

Figure 2.5: P-V characteristic of the PV cell [16]

Finally in order to measure the photovoltaic cells output power the following standard test conditions are established internationally. The irradiance level is 1000 W/m², with the reference air mass 1.5 solar spectral irradiance distributions and cell or module junction temperature of 25°C.

2.8. Solar Radiation Estimations

For any solar based system design, the most important factors are the position of the sun in the sky, the slope and orientation of a collecting surface, and obstruction and reflection properties of neighboring structures. Figure 2.6 shows the geometry describing orientation of a collector and position of the sun in the sky.

A point on the earth’s surface is expressed by its latitude and longitude. The angle between the collector surface and the horizontal is called slope, β (with $0^0 < \beta < 90^0$ for a surface facing towards the equator; $90^0 < \beta < 180^0$ for a surface facing away from the equator). Surface azimuth angle, γ is the angle between the normal to the surface and the local longitude meridian, projected on the horizontal plane. In either hemisphere, γ equals 0^0 for a surface facing due south, 180^0 due north, 0^0 to 180^0 for a surface facing westward and 0^0 to - 80^0 eastward. For a horizontal surface, γ is always 0^0.

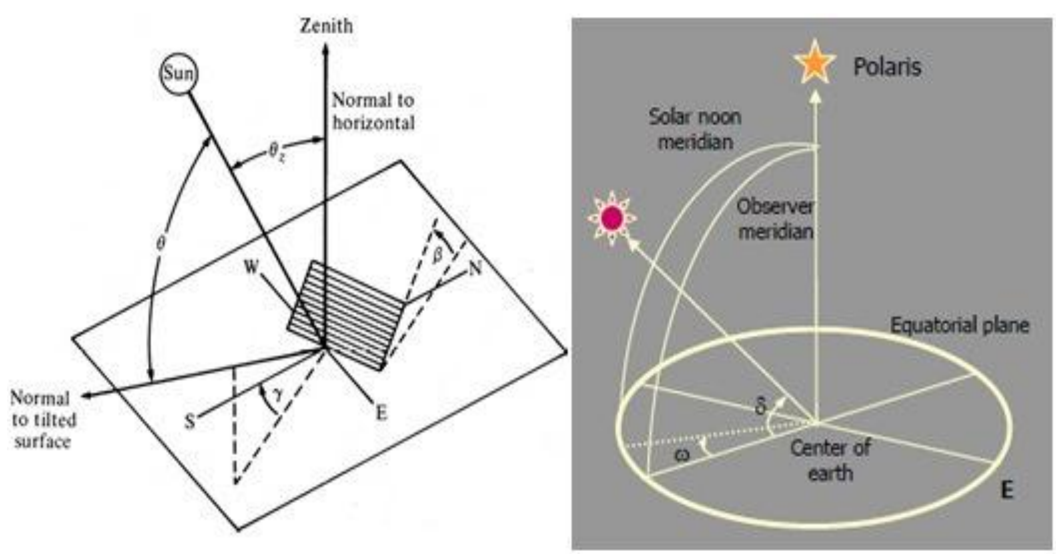

Figure 2.6: Geometry of solar collector and location of sun relative to earth [19]

Location of the sun in the sky, relative to a point on the ground, can be defined in terms of two angles, the solar altitude, α_s (or its complement the solar zenith angle,θ_z) and the solar azimuth

γ_s. Solar altitude, α_s, angle of solar beam to the horizontal. Solar azimuth, γ_s is the angle between the solar beam and the longitude meridian projected on the horizontal plane. Sign convention is the same as for surface azimuth angle (γ). Solar altitude and solar azimuth are functions of location (latitude, ϕ), time of the year (declination angle, δ) and time of the day (hour angle, ω). Solar declination angle (δ) is the angle between the earth's equatorial plane and the earth sun line. Solar hour angle ω is the angle Earth has rotated since solar noon. The relation between these angles is given below [4, 17, 19].

$$\delta = 23.45 sin\left(360\frac{284+n_d}{365}\right) \tag{2.5}$$

Where, δ = solar declination angle (^{0})

n_d = day number of the year starting at January 1st as 1

$$\omega = (12 - t_L)15^{\circ} \tag{2.6}$$

Where, t_L=local solar time in hours.

ω = solar hour angle (^{0})

$$sin(\alpha) = sin(\phi)sin(\delta) + cos(\phi)cos(\delta)cos(\omega) \tag{2.7}$$

Where, α_s= solar altitude (^{0})

ϕ = latitude (^{0})

$$\sin(\gamma_s) = \frac{cos(\delta)sin(\omega)}{cos(\alpha_s)} \tag{2.8}$$

Where, γ_s= solar azimuth (^{0})

The sunset/sunrise angle is given by

$$\omega_s = cos^{-1}\left(-tan(\phi)tan(\delta)\right) \tag{2.9}$$

The angle of incident θ_i is the angle between the solar beam and normal to the solar panel which is given by:

$$cos(\theta_i) = sin(\delta)sin(\phi)cos(\beta) - sin(\delta)cos(\phi)sin(\beta)cos(\gamma) + cos(\delta)cos(\phi)cos(\beta)cos(\omega) + cos(\delta)sin(\phi)sin(\beta)cos(\gamma)cos(\omega) + cos(\delta)sin(\beta)sin(\gamma)sin(\omega) \quad ...(2.10)$$

The intensity of solar radiation incident per unit area exposed normally to the sun's rays at the average sun-earth distance (about $1.5x10^{11}$m), measured outside the earth's atmosphere is called the solar constant, G_{sc} (1367 W/m^2) [17, 20]. The intensity of radiation received outside the earth's atmosphere varies as the inverse square of the earth-sun distance and can be expressed in relation to time of the year. The extraterrestrial irradiance on a surface at normal incidence (G_{on}) may be expressed as:

$$G_{on} = G_{sc}\left[1 + 0.003cos\frac{2\pi n_d}{365}\right] \quad (2.11)$$

The extraterrestrial irradiance incident on a horizontal plane at an arbitrary angle of incidence is given by,

$$G_o = G_{on}\cos(\theta_z) \quad (2.12)$$

Where θ_z=zenith angle (angle between the sun and the vertical line from a point on earth) which equals to the incident angle of a horizontal surface at the point of interest.

The whole daily extraterrestrial radiation, Ho from the sunrise to the sunset can be calculated as follows:

$$H_o = \frac{24*3600*G_{sc}}{\pi}\left(1 + 0.033 * cos\left(\frac{360N}{365}\right)\right) * \left(cos\phi cos\delta sin\omega_s + \frac{\pi\omega_s}{180}sin\phi sin\delta\right) \quad (2.13)$$

Where, $N \rightarrow$Day number starting from January 1st as 1,

$G_{SC} \rightarrow$1367 W/m^2, the solar constant,

$\phi \rightarrow$Latitude of the location (14^0),

$\delta \rightarrow$Declination angle (^{0}) given by equation (2.4).

$\omega_s \rightarrow$ Sunset hour angle (^{0})

Ideally, the data required to predict the solar potential of any site are several years of measurements of irradiance on the proposed collector plane. These are rarely available, so the required data have to be estimated from meteorological data available either (i) from the site, or (ii) from some nearby site having similar irradiance, or (iii) from an official solar atlas or database [19]. Here, the sunshine duration data from the nearby station is used to estimate the monthly average solar radiation using the following angstrom type equation [5, 6, 21 and 22].

$$\frac{H}{H_o} = a + b\frac{n}{N_s} \tag{2.14}$$

Where, $H \rightarrow$ monthly average daily radiation on horizontal surface (MJ/m^2)

$H_o \rightarrow$ monthly average daily extraterrestrial radiation on a horizontal surface (MJ/m^2)

$N_s \rightarrow$ the maximum possible daily hours of bright sunshine given by equation

$n \rightarrow$monthly average daily number of hours of bright sunshine a and b are regression coefficients having average value of a =0.30 and b=0.50 [4].

The day length, N_s, is the maximum possible daily sunshine hour is given by equation 1.15.

$$N_s = \frac{2}{15} \times \omega_s \tag{2.15}$$

2.9. Solar Energy Resource in Ethiopia

Ethiopia receives 4.55 to 6.5 kWh/m^2/day annual average of solar isolation throughout the country [2, 4, 8, and 23]. This varies significantly during the year, ranging from a minimum of 4.55 kWh/m^2 in July to a maximum of 6.55 kWh/m^2 in February and March. Other literatures describe the yearly average radiation to be in the range from 4.25 kWh/m^2 in the areas of Itang in the Gambella regional state (western Ethiopia), to 6.25 kWh/m^2 around Adigrat in the Tigray regional state (northern Ethiopia) [2, 21].

2.9.1. Solar Energy Assessment of Adigrat District

The assessment of the potential for solar radiation of the selected area is done by taking data from different sources. These are National Metrological Service Agency of Ethiopia (NMSA), NASA, SWERA and as well as data assessed by Mulugeta and Drake for the regions of the country. At the first approach, the data taken from the National Metrological Service Agency is analyzed using mathematical approach based on the sunshine duration collected on the past five consecutive years starting from 2005 to 2009. The sunshine duration data taken from the National Metrological Agency of Ethiopia, Mekele branch, is converted into solar radiation using Angstrom Radiation-Sunshine Relation [4]. Therefore, for calculating the radiation in KWh/m^2 from the sunshine duration, the values for the regression coefficients ɑ and b are taken to be 0.30 and 0.50 respectively [4]. Finally, this result is compared with the data taken from NASA and SWERA, and it is found that the annual average solar radiation obtained from NMSA is $6.21KWh/m^2$ and from NASA is 5.94 KWh/m^2. For this study, the calculated monthly average daily radiation summarized in Table 2.1 is used for modeling the hybrid system. The monthly average solar radiation of Adigrat for the data taken from NMSA and NASA is shown on Table 2.1 and Table 2.2 respectively.

Table 2.1: Solar radiation of Adigrat in KWh/m^2/day data from NMSA

Year	J	F	M	A	M	J	J	A	S	N	O	D
2005	5.37	6.81	6.64	7.17	7.12	7.22	6.13	6.17	6.46	6.45	5.99	5.91
2006	5.62	6.61	6.60	6.90	6.98	6.65	5.56	5.59	5.85	6.13	5.81	5.34
2007	5.24	6.61	7.20	6.90	7.12	6.47	5.78	6.08	6.15	6.33	5.65	5.55
2008	5.08	6.85	7.11	7.23	6.98	6.69	5.87	6.04	6.20	6.21	6.34	5.50
2009	5.43	6.17	6.73	6.99	7.70	7.05	5.25	5.68	6.33	6.04	6.33	4.94
monthly average	**5.35**	**6.61**	**6.86**	**7.15**	**7.18**	**6.82**	**5.72**	**5.91**	**6.20**	**6.20**	**6.02**	**5.45**
Annual Average in KWh/m^2/day												**6.29**

Table 2.2: Solar radiation of Adigrat in KWh/m^2/day data from NASA

	Jan	Feb	Mar	Apr	May	Jun	Jul	Aug	Sep	Oct	Nov	Dec	Annual Average
22 year Average	5.71	6.08	6.33	6.66	6.49	6.10	5.49	5.58	5.30	5.95	6.01	5.78	5.94

CHAPTER THREE

WIND ENERGY SYSTEMS AND WND ENERGY RESOURCES

3.1. Introduction

Winds are produced by uneven solar heating of the earth's land and sea surfaces. Thus, they are a form of "solar" energy. On average, the ratio of total wind power to incident solar power is on the order of two present, reflecting a balance between input and dissipation by turbulence and drag on the surface.

Wind is the movement of air caused by the irregular heating of the Earth's surface. It happens at all scales, from local breezes created by heating of land surfaces that lasts some minutes, to global winds caused from solar heating of the Earth. Wind power is the transformation of wind energy into more utile forms, typically electricity using wind turbines [24].

3.2. Historical Uses of Wind

Wind energy is one of the oldest sources of energy used by humankind, comparable only to the use of animal force and biomass [25]. Some 5000 yrs ago wind was used to sail ships in the Nile. Many civilizations used wind power for transportation and other purposes: The Europeans used it to accomplish some mechanical works such as grind grains and pump water in the 1700s and 1800s. The first wind turbine used to generate electricity was installed in U.S in 1890 [16]. However, for much of the twentieth century there was small interest in using wind energy other than for battery charging for distant dwellings. These low-power systems were quickly replaced once the electricity grid became available. The sudden increases in the price of oil in 1973 stimulated a number of research, development and demonstrations of wind turbines and other alternative energy technologies in different countries [26].

3.3. Distribution of Wind Speed

The distribution of wind is expressed by Weibull distribution over a certain period of time at a particular site. The Weibull probability density function (PDF) is given by equation (3.1) [27].

$$f(u) = \frac{k}{c}\left(\frac{u}{c}\right)^{k-1} exp\left[-\frac{u^k}{c}\right] \qquad (3.1)$$

Where, u = the wind speed,

k = a constant known as shape factor, as the value of k increases the curve will have a sharper peak

c = a scale parameter in m/s; the larger the scale parameter, the more spread out the distribution.

The area under the curve is always unity. The power density can in this case be expressed by equation (3.2).

$$P/_{A} = \frac{1}{2}\sum_{j=1}^{n} \rho {V_j}^3 f_j \qquad (3.2)$$

where V_j is the median velocity in class j and f_j is the frequency of occurrence in the same class. For k = 2 the Weibull PDF is commonly known as the Rayleigh density function in which case equation (3.1) may be rewritten as in equation (3.3).

$$f(u) = \frac{2u}{c^2} exp\left[-\left(\frac{u}{c}\right)^2\right] \qquad (3.3)$$

3.4. Wind Turbines

A wind turbine is a machine that converts the kinetic energy from the wind into mechanical energy. If the mechanical energy is used directly by machinery, such as a pump or grinding stones, the machine is usually called a windmill. If the mechanical energy is then converted to electricity, the machine is called a wind generator [24].

There are a number of different wind turbine types available. The horizontal axis turbine, HAWT is by far the most common type of turbine. They come in two different types: the upwind, which face the wind (tower behind rotor) and the downwind arrangement that works away from the wind (tower in front). Another kind of turbine is the vertical axis, VAWT arrangement that uses drag and lift as the driving forces; the horizontal also uses drag and lift, but in other proportions.

The advantages with upwind turbines are that the tower does not act as an obstacle for the wind hitting the rotor. Despite this, the flow behind the passing blade is affected by the tower and causes a slight drop in power. When the blade passes the tower it also decreases the drag on the construction which can cause an on / off bending process causing fatigue stress. This has of course been taking into account when designing the turbine. The upwind design needs a control system that helps the nacelle turn straight to the wind. In downwind turbines, the tower shades a rotor blade each time it passes by and causes greater power losses compared to the upwind design. An advantage with downwind turbines is that the nacelle is self-adjusting and is not in need of a control system. One drawback with this is the problem with untwisting the cable inside when the nacelle has turned same direction repeatedly. The VAWT´s are not as commercial and economically competitive as the HAWT´s. Some of the VAWT types suffer from low efficiency due to design difficulties as well as the problem with operation close to the ground. Parts of the vertical turbines will therefore receive low quality winds causing power losses. To keep the construction upright it also needs to be supported with guy cables attached to the ground. The vertical turbine is not in need of yaw control, which of course is an advantage and the wind always hits the turbine tangentially [28].

The modern wind turbine is a sophisticated piece of machinery with aerodynamically designed rotor and efficient power generation, transmission and regulation components. The size of these turbines ranges from a few Watts (Small Wind Turbines) to several Million Watts (Large Wind Turbines). The modern trend in the wind industry is to go for bigger units of several MW capacities in places where the wind is favorable, as the system scaling up can reduce the unit cost of wind-generated electricity. Most of today's commercial machines are horizontal axis wind turbines (HAWT) with three bladed rotors.

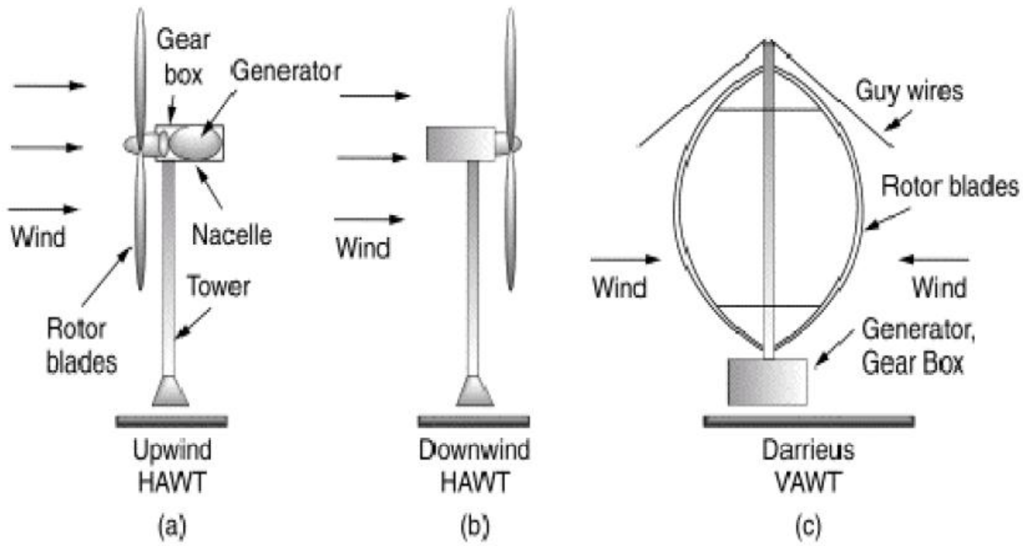

Figure 3.1: Horizontal axis wind turbines (HAWT) are either upwind machine or down wind machines

(a) Upwind machine (b) Or down wind machines (c). Vertical axis wind turbines (VAWT) accept wind from any direction [29].

3.4.1. Wind Turbines Components

The most common turbine type is the horizontal axis wind turbine. A cut-view (Figure 3.2) helps the reader to get familiar with the components of a wind turbine.

Anemometer:

Measures the wind speed and transmits wind speed data to the controller.

Hub:

Hub is the connection point for the rotor blades and the low speed shaft.

Gear box:

Gears connect the low-speed shaft to the high-speed shaft and increase the rotational speeds from about 30 to 60 rotations per minute (rpm) to about 1200 to 1500 rpm, the rotational speed required by most generators to produce electricity. The gear box is a costly (and heavy) part of the wind turbine and engineers are exploring "direct-drive" generators that operate at lower rotational speeds and don't need gear boxes specially for small scale wind turbines.

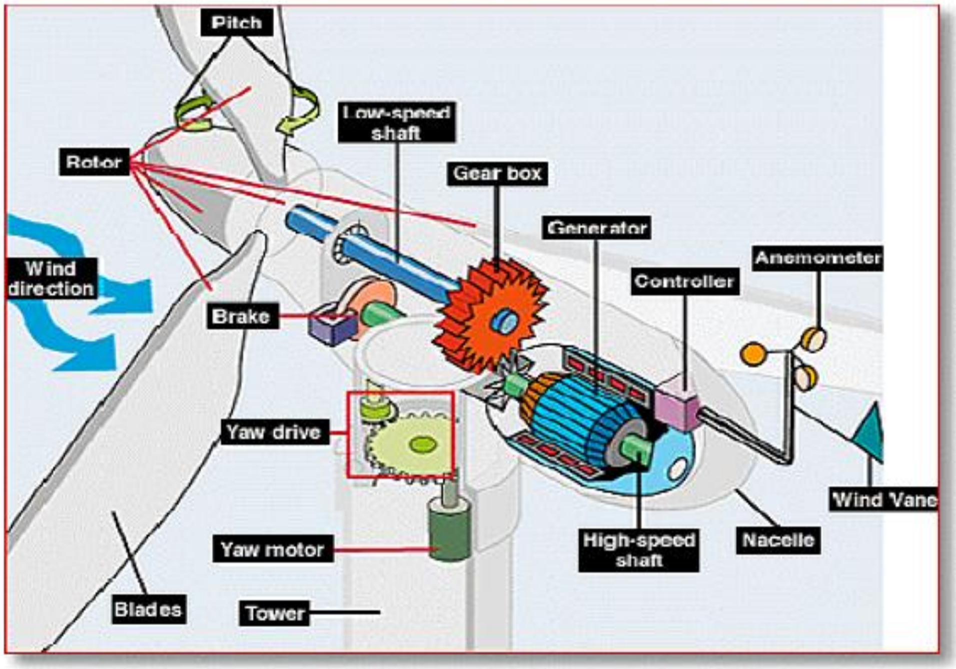

Figure 3.2: Cut-View Wind Turbine [15]

Generator:

The generator is connected to the high-speed shaft and is the component of the system that converts the rotational energy of the shaft into an electrical output.

Tower of wind power generation:

The tower is used to support the nacelle and rotor blades and typically made of rolled, tubular steel, and built and shipped in sections because of its size and weight. Common tubular towers incorporate a ladder within the hollow structure to provide maintenance access. Small -scale towers range in height from 24-35m and its weight depends on the material from where it is manufactured.

Nacelle:

The rotor attaches to the nacelle, which sits top the tower and includes the gear box, low- and high-speed shafts, generator, controller, and brake. A cover protects the components inside the nacelle. Some nacelles are large enough for a technician to stand inside while working rotor in emergencies.

Controller:

The controller starts up the machine at wind speeds of about 3.5 to 7.2 meters per sec (m/s) and shuts off the machine at about 30 m/s.

High-speed shaft:

Drives the generator.

Low-speed shaft:

The rotor turns the low-speed shaft at about 30 to 60 RPM.

Pitch:

Blades are turned, or pitched, out of the wind to keep the rotor from turning in winds that are too high or too low to produce electricity.

Rotor:

The blades and the hub together are called the rotor.

Tower:

Towers are made from tubular steel or steel lattice. Because wind speed increases with height, taller towers enable turbines to capture more energy and generate more electricity.

Yaw drive:

Upwind turbines face into the wind; the yaw drive is used to keep the rotor facing into the wind as the wind direction changes. Downwind turbines don't require a yaw drive; the wind blows the rotor downwind.

Yaw motor:

Powers the yaw drive.

Electronic equipment:

Such as controls, electrical cables, ground support equipment and interconnection equipment.

3.4.2. Workings Principles of Wind Turbines

The blade, using aerodynamic lift, capture energy from wind in order to turn the shaft. In small wind turbines the shaft usually drives the generator directly. The generator converts the mechanical energy into electricity. The shaft power causes coils to spin past alternate poles of magnets allowing electric current to flow. If a permanent magnet device is being used the opposite occur: current flow as magnets spin past coil windings. Most small wind turbines use a permanent magnet alternator. Large wind turbines usually use either induction generator or a synchronous generator. In addition, in large wind turbines the shaft connected to the generator via a gearbox those steps up the rotational speed for the generator.

3.5. Wind Energy Extraction by HAWT

The energy of wind is extracted by using appropriate wind turbine. The wind energy is tapped by the wind turbine which converts the kinetic energy of the wind into mechanical shaft energy. The rotational energy is converted into electrical energy through the transmission system. The transmission system consists of the rotor shaft with bearings, brake(s), an optional gearbox, as well as a generator and optional clutches. The energy available in the wind can be expressed using equation (3.4).

$$P_w = \frac{1}{2}\rho A v^3 \qquad (3.4)$$

Where, ρ =Density of air (kg/m^3)

A = the swept area (m^2)

P_w = power in the wind (W)

v =instantaneous wind velocity (m/s)

Energy conversion from free-flowing fluid streams is limited because full energy extraction implies decrease of fluid velocity (decrease of kinetic energy of the stream), down to zero which is impossible. Some fluid may not pass through the turbine and may simply flow around it (bypass it). This limitation is expressed in terms of Betz limit defined by the power coefficient C_p as given by equation (3.5).

$$C_p = \frac{Rotor-power}{power-in-the-wind} \qquad (3.5)$$

The power coefficient, C_P, is a function of the axial induction factor. The optimum of this function (which is a maximum value for C_P) is 0.5926 (=16/27) [19, 20, 21]. Thus the electrical power output from the wind turbine can be expressed by equation (3.6).

$$P_w out = \eta_t c_p {}^1\!/_2 \rho A v^3 \qquad (3.6)$$

Where, P_w *out* = output power of wind turbine

η_t = Overall efficiency of the transmission system/power train

C_p = the power coefficient

The power coefficient and efficiency of wind turbines vary greatly from manufactures to manufacturers. As a result, the power output of wind turbines vary from turbine to turbine and is given by power curve which plots the output power of a turbine against wind speed (see Figure 3.3).

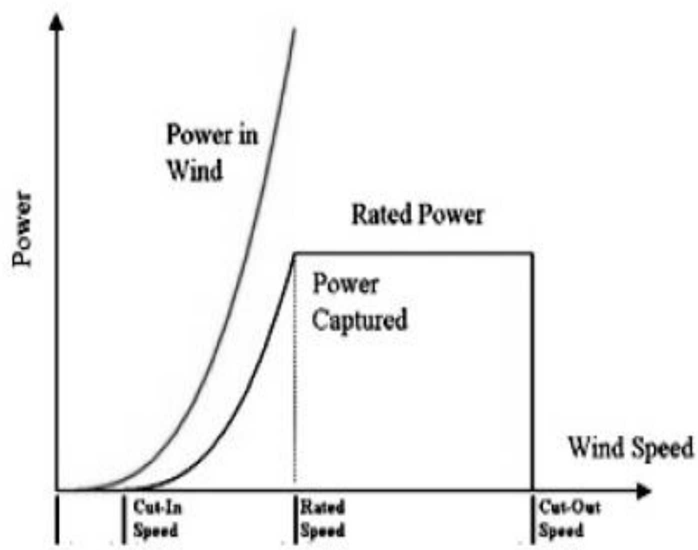

Figure 3.3: General power curve of wind turbine [21]

The wind speed at which wind turbine starts generating electrical power is called the cut- in speed. The rated wind speed is the wind speed at which the turbine operates at its maximum efficiency of energy conversion. Rated power is the power output at the wind speed which is equal to, or above, the rated speed. The cut-out speed is the wind speed at which the turbine may be shut down to protect the rotor and drive train machinery from damage, or high wind stalling characteristics.

3.6. Wind Turbines Power Control Mechanism

All wind turbines are designed with some sort of power control. There are different ways to control aerodynamic forces on the turbine rotor and thus to limit the power in very high wind speeds in order to avoid damage to the turbine. There are three commonly used types of power control in the industry [30].

- Stall Control
- Pitch Control
- Active stall regulation

The simplest, most robust and cheapest control method is the stall control (also called passive control), where the blades are bolted onto the hub at a fixed angle. The fixed-blade pitch is chosen so that the turbine reaches its maximum or rated power at the desired wind speed. The design of the rotor aerodynamics causes the rotor to stall (lose power) when the wind speed exceeds a certain level which limits the aerodynamic power on the blades.

Another type of control is pitch control, where the blades can be turned out or into the wind as the power output becomes too high or too low, respectively. Generally, the advantages of this type of control are good power control, increased energy capture, assisted startup and emergency stop. The pitch change system has to act rapidly. From an electrical point of view, good power control means that at high wind speeds the mean value of the power output is kept close to the rated power of the generator. The extra complexity arising from the pitch mechanism and the higher power fluctuations at high wind speeds can be mentioned as the demerits of this control scheme.

The third possible control strategy is the active stall control, in which the stall of the blade is actively controlled by pitching the blades. At low wind speeds, the blades are pitched similar to a pitch-controlled wind turbine, in order to achieve maximum efficiency. At high wind speeds, the blades go into a deeper stall by being pitched slightly into the direction opposite to that of a pitch-controlled turbine. The active stall wind turbine achieves a smoother limited power, without high power fluctuations as in the case of pitch-controlled wind turbines. This control type has the advantage of being able to compensate variation in air density and inherits the advantages of both pitch and stall control mechanisms.

3.7. Wind Energy Resources

Wind resource is the most important element in determining turbine performance at a given place. The energy that can be extracted from a wind stream is proportional to the cube of its velocity. In addition, the wind resource itself is intermittent. It varies with year, season, and time of day, elevation above ground, and form of terrain. Proper choice of site which is free from large obstructions, improves wind turbines performance.

3.7.1. Wind Speed Measurement

The wind speed is measured with an instrument called an anemometer. These instruments come in several types. The most common type is a cup anemometer which has three or four cups attached to a rotating shaft. When the wind hits the anemometer, the cups and the shaft rotate. The angular speed of the spinning shaft is calibrated in terms of the linear speed of the wind. Normally, the anemometer is fitted with a wind vane to detect the wind direction. A data logger collects wind speed and wind direction data from the anemometer and wind vane respectively.

It is very important that the measuring equipment is set high enough to avoid turbulence created by trees, buildings or other obstructions. Readings would be most useful if they have been taken at hub height where the wind turbine is going to be installed [24].

If the measurement of wind speed was not made at the wind turbine hub height (in this case it is 10 m) it is important to adjust the measured wind speed to the hub height. This can be done using either the logarithmic law, which assumes that the wind speed is proportional to the logarithm of the height above ground, or the power law, which assumes that the wind speed varies exponentially with height. Using the logarithmic law the wind speed at a certain height above ground level can be given as follows [13]:

$$v(\mathrm{z}).\ln\left(\frac{\mathrm{z_r}}{\mathrm{z_o}}\right) = v(\mathrm{z_r}).\ln\left(\frac{\mathrm{z}}{\mathrm{z_o}}\right) \qquad (3.7)$$

Where, Z_r →Reference height (m)

Z → Height where wind speed is to be determined (m)

Z_0 → Measure of surface roughness (0.1 to 0.25 for crop land)

$v(z)$ →Wind speed at height of Z m (m/s)

$v(z_r)$ → Wind speed at the reference height (m/s)

Using power law the wind speed at a certain height above ground level can be given as follows [16]:

$$v_2 = v_1 \left(\frac{h_2}{h_1}\right)^{\alpha} \tag{3.8}$$

Where: v_1 is wind speed measured at the reference height h_1 (m/s), v_2 is wind speed estimated at height h_2 (m/s), and α is ground surface friction coefficient.

Table 3.1: Friction Coefficient α of Various Terrains [16]

Terrain Type	Friction coefficient α
Lake, ocean, and smooth, hard ground	0.10
Foot-high grass on level ground	0.15
Tall crops, hedges, and shrubs	0.20
Wooded country with many trees	0.25
Small town with some trees and shrubs	0.30
City area with tall buildings	0.40

3.8. Wind Resource in Ethiopia

Ethiopia has exploitable reserve of 100 GW wind energy with an average speed of 3.5 – 5.5 m/s, flowing for 6 hours/day. There are two basic zones with homogenous periodicity separated by the rift valley. In the first of these, covering most of the highland plateaus, there are two well-defined wind speed maximal occurring, respectively, between March and May and between September and November. In the second zone, covering most of the Ogaden and the eastern lowlands, average wind velocity reaches maximum values between May and August [5, 7, 8, 22, 23 and 30]. Currently two projects are constructed, one Ashegoda wind park (near Mekele) of 120MW and the other Adama Wind Park of nearly 51MW.

3.8.1. Wind Potential Assessment in the Study Area

The resource assessment for the wind potential is done by taking the data's only from NASA. This is because of the absence of full data regarding wind speed in the National Metrological Service Agency of Ethiopia and in SWERA. Therefore, the annual average wind speed for Adigrat, which is located at latitude of 14°00' N and longitude of 39°27' E, is found to be 4.42 m/s at a height of 10m. This value is used as an input to the wind resource in modeling the hybrid system. This data can be extrapolated to the selected wind turbine height using equation 3.8 [5,6]. The value of Z_0 is taken as 0.1 [13]. Table 3.2 summarizes the wind speed at 10 m and 25 m heights.

Table 3.2: Monthly average wind speed (m/s) at the site from NASA

	Jan	Feb	Mar	Apr	May	Jun	Jul	Aug	Sep	Oct	Nov	Dec	Av.
NASA(10m)	4.62	4.65	4.68	4.30	3.66	5.14	5.68	5.25	4.33	3.20	3.52	4.07	4.42
At 25m	5.54	5.58	5.61	5.16	4.39	6.16	6.81	6.29	5.19	3.84	4.22	4.88	5.31

CHAPTER FOUR

BIOGAS ENERGY SYSTEMS AND BIOGAS ENERGY RESOURCES

4.1. Introduction

Biogas is produced by anaerobic digestion with anaerobic bacteria or fermentation of biodegradable materials such as manure, sewage, municipal waste, plant material, and crops . It is a renewable energy source, like solar and wind energy which comprises primarily of methane (CH_4) and carbon dioxide (CO_2) and may have small amounts of hydrogen sulphide (H_2S), moisture and siloxanes. Additionally, biogas can be produced from regionally available raw materials such as recycled waste and is environmentally friendly [31].

The gases methane, hydrogen, and carbon monoxide (CO) can be combusted or oxidized with oxygen. This releases biogas to be used as a fuel. Biogas can be used as a fuel for any heating purpose, such as cooking. It can also be used in a gas engine to convert the energy in the gas into electricity and heat [32].

Biogas can be compressed; the same way natural gas is compressed to compressed natural gas (CNG) and used to power motor vehicles [33]. Biogas can also be cleaned and upgraded to natural gas standards when it becomes Biomethane and can be used in the place of natural gas to run simple or combined cycle power plants to generate electricity or used as a heat source for home or industrial use. The average calorific value of biogas is about 21-23.5 MJ/m^3, so that $1m^3$ of biogas corresponds to 0.5-0.6 l diesel fuel or about 6 kWh. However, when we convert biogas to electricity, in a biogas powered electric generator, we get about 2kWh of useable electricity, and the rest turns into heat which can also be used for heating applications [34].

A biogas plant is the name often given to anaerobic digester that treats farm wastes or energy crops. These plants can be fed with any of the biodegradable materials. During the process, an air-tight tank transforms biomass waste into methane, producing renewable energy that can be used for heating, electricity, and other operations. The typical compositions of biogas are summarized in the Table 4.1 below.

Table 4.1: Composition of biogas

Compound	Chemical formula	%
Methane	CH_4	50-75
Carbon dioxide	CO_2	25-50
Nitrogen	N_2	0-10
Hydrogen	H_2	0-1
Hydrogen sulfide	H_2S	0-3

Biogas could potentially help reduce global climate change. Normally, manure that is left to decompose releases two main gases that cause global climate change: nitrous dioxide and methane. Nitrous dioxide (NO_2) warms the atmosphere 310 times more than carbon dioxide and methane 21 times more than carbon dioxide. By converting cow manure into methane biogas instead of letting it decompose, we would be able to reduce global warming gases by ninety-nine million metric tons or four percent [35].

4.2. The Biochemical Process of AD

Anaerobic digestion is a multiple bio-process, of which four main steps can be identified [36], namely hydrolysis, acidogenesis, acetogenesis and methanogenesis shown Figure 4.1 below.

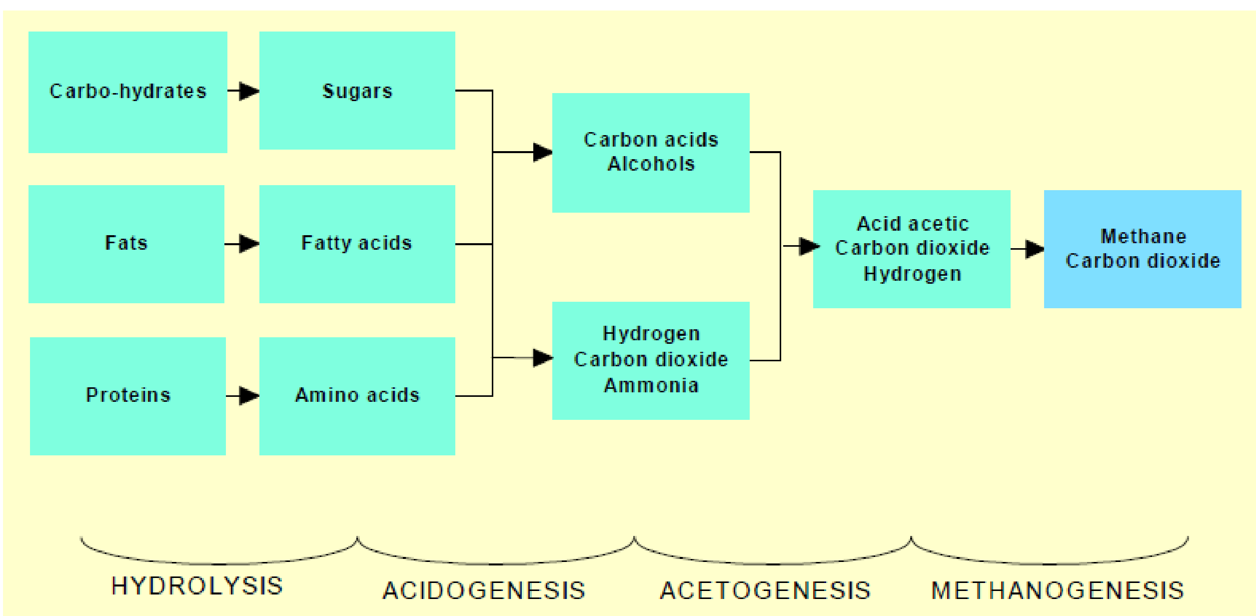

Figure 4.1: The main process steps of anaerobic digestion [37]

The process steps shown above in Figure 4.1 run parallel in time and space, in the digester tank. The speed of the total decomposition process is determined by the slowest reaction of the chain. In the case of biogas plants, processing vegetable substrates containing cellulose, hemi-cellulose and lignin, hydrolysis is the speed determining process. During hydrolysis, relatively small amounts of biogas are produced. Biogas production reaches its peak during methanogenesis. The brief notes of the four main process steps of AD: hydrolysis, acidogenesis, acetogenesis, and methanogenesis are given below.

4.2.1. Hydrolysis

In this step, complex organic matter (polymers) is decomposed into smaller units (mono- and oligomers). During hydrolysis, polymers like carbohydrates, lipids, nucleic acids and proteins are converted into glucose, glycerol, purines and pyridines. Hydrolytic microorganisms excrete hydrolytic enzymes, converting biopolymers into simpler and soluble compounds as it is shown below [36, 38].

$$\text{Lipids} \xrightarrow{\text{Lipase}} \text{fatty acids, glycerol}$$

$$\text{Polysaccharide} \xrightarrow{\text{cellulase, cellobiase, xylanase,amylase}} \text{monosaccharide}$$

$$\text{Proteins} \xrightarrow{\text{protease}} \text{amino acids}$$

4.2.2. Acidogenesis

During acidogenesis, the products of hydrolysis are converted by acidogenic (fermentative) bacteria into methanogenic substrates. Simple sugars, amino acids and fatty acids are degraded into acetate, carbon dioxide and hydrogen (70%) as well as into volatile fatty acids (VFA) and alcohols (30%) [36, 38].

4.2.3. Acetogenesis

Products from acidogenesis, which cannot be directly converted to methane by methanogenic bacteria, are converted into methanogenic substrates during acetogenesis. VFA and alcohols are oxidized into methanogenic substrates like acetate, hydrogen and carbon dioxide. VFA, with carbon chains longer than two units and alcohols, with carbon chains longer than one unit, are oxidized into acetate and hydrogen. The production of hydrogen increases the hydrogen partial pressure. This can be regarded as a waste product of acetogenesis and inhibits the metabolism of the acetogenic bacteria. During methanogenesis, hydrogen is converted into methane. Acetogenesis and methanogenesis usually run parallel, as symbiosis of two groups of organisms [36, 38].

4.2.4. Methanogenesis

The production of methane and carbon dioxide from intermediate products is carried out by methanogenic bacteria. 70% of the formed methane originates from acetate, while the remaining 30% is produced from conversion of hydrogen (H) and carbon dioxide (CO2), according to the following equations:

$$\text{Acetic acid} \xrightarrow{\text{methanogenic bacteria}} \text{methane + carbon dioxide}$$

$$\text{Hydrogen + carbon dioxide} \xrightarrow{\text{methanogenic bacteria}} \text{methane +water}$$

Methanogenesis is a critical step in the entire anaerobic digestion process, as it is the slowest biochemical reaction of the process. Methanogenesis is severely influenced by operation conditions. Composition of feedstock, feeding rate, temperature, and pH are examples of factors influencing the methanogenesis process. Digester overloading, temperature changes or large entry of oxygen can result in termination of methane production [36, 38].

4.3. Factors Affecting Anaerobic Digestion Process (Methanogenesis)

The efficiency of anaerobic digestion is influenced by some critical parameters, thus it is crucial that appropriate conditions for anaerobic microorganisms are provided. The growth and activity of anaerobic microorganisms is significantly influenced by conditions such as exclusion of oxygen, constant temperature, pH-value, nutrient supply, stirring intensity as well as presence and amount of inhibitors (e.g. ammonia) [39].

4.3.1. Anaerobic Environment

As mentioned earlier, the methanogenesis need an oxygen-free environment – they are obligatory anaerobic. A biogas reactor therefore has to be airtight. The small amount of oxygen dissolved in the liquid/biomass fed to the plant is quickly used up by, for example, aerobic bacteria that must have oxygen, or by facultative anaerobic bacteria that can use oxygen for their respiration, if it is present [39].

4.3.2. Temperature

The methanogenesis process can take place at different temperatures, divided into three temperature ranges: psychrophilic (below 25^0C), mesophilic (25^0C – 45^0C), and thermophilic (45^0C – 70^0C). There is a direct relation between the process temperature and the HRT (Table 4.2).The methanogenesis are inactive in extreme high and low temperatures. The optimum temperature is 35°C. When the ambient temperature goes down to 10°C, gas production virtually stops. Satisfactory gas production takes place in the so called mesophilic range; between 25ºC to 30°C. Proper insulation on top of the digester, helps to increase gas production in the cold season. When the ambient temperature is 30°C or less, the average temperature within the field will than remain about 4ºC above the ambient temperature [38, 39].

Table 4.2: Thermal stage and typical retention times

Thermal stage	Process temperatures	Minimum retention time
Psychrophilic	< 20 °C	70 to 80 days
Mesophilic	30 to 42 °C	30 to 40 days
Thermophilic	43 to 55 °C	15 to 20 days

Many modern biogas plants operate at thermophilic process temperatures as the thermophilic process provides many advantages, compared to mesophilic and psychrophilic processes:

- effective destruction of pathogens
- higher grow rate of methanogenic bacteria at higher temperature

- reduced retention time, making the process faster and more efficient
- improved digestibility and availability of substrates
- better degradation of solid substrates and better substrate utilization
- better possibility for separating liquid and solid fractions

Operation temperature influences the toxicity of ammonia. Ammonia toxicity increases with increasing temperature and can be relieved by decreasing the process temperature. However, when decreasing the temperature to 50°C or below, the growth rate of the thermophilic microorganisms will drop drastically, and a risk of washout of the microbial population can occur, due to a growth rate lower than the actual HRT [40]. This means that a well-functioning thermophilic digester can be loaded to a higher degree or operated at a lower HRT than an e.g. mesophilic one because of the growth rates of thermophilic organisms (Figure 4.2). Experience shows that at high loading or at low HRT, a thermophilic operated digester has higher gas yield and higher conversion rates than a mesophilic digester.

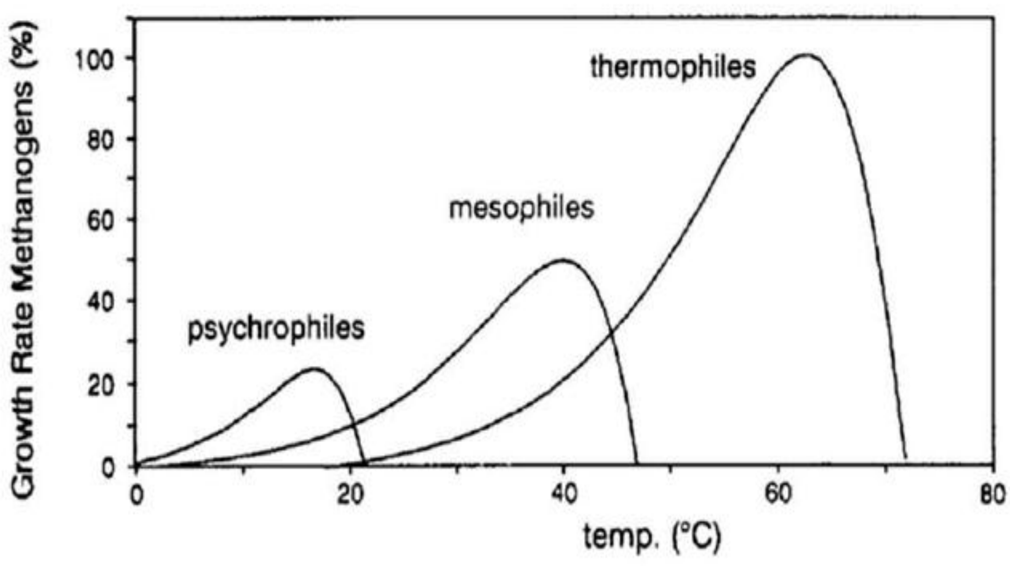

Figure 4.2: Relative growth rates of methanogenesis [40]

4.3.3. pH-values and optimum intervals

The pH-value is the measure of acidity/alkalinity of a solution (respectively of substrate mixture, in the case of AD) and is expressed in parts per million (ppm). The pH value of the AD substrate influences the growth of methanogenic microorganisms and affects the dissociation of some compounds of importance for the AD process (ammonia, sulphide, organic acids). The micro-organism requires a neutral or mildly alkaline environment-a too acidic or too alkaline environment will be detrimental. Ideal pH value is 7.0-8.0 but can go up or down by further 0.5.The pH value depends on the ratio of acidity and alkalinity and the carbon dioxide content in the biogas digester, the determining factor being the density of acids. Experience shows that methane formation takes place within a relatively narrow pH interval, from about 5.5 to 8.5, with an optimum interval between 7.0-8.0 for most methanogenesis. Acidogenic microorganisms usually have lower value of optimum pH.

The optimum pH interval for mesophilic digestion is between 6.5 and 8.0 and the process is severely inhibited if the pH-value decreases below 6.0 or rises above 8.3. The solubility of carbon dioxide in water decreases at increasing temperature. The pH-value in thermophilic digesters is therefore higher than in mesophilic ones, as dissolved carbon dioxide forms carbonic acid by reaction with water [39].

4.3.4. Volatile fatty acids (VFA)

The stability of the anaerobic digestion process is reflected by the concentration of intermediate products like the VFA. The VFA are intermediate compounds (acetate, propionate, butyrate, lactate), produced during acidogenesis, with a carbon chain of up to six atoms. In most cases, AD process instability will lead to accumulation of VFA inside the digester, which can lead furthermore to a drop of pH-value. However, the accumulation of VFA will not always be expressed by a drop of pH value, due to the buffer capacity of the digester, through the biomass types contained in it. Animal manure e.g. has a surplus of alkalinity, which means that the VFA accumulation should exceed a certain level, before this can be detected due to significant decrease of pH value. At such point, the VFA concentration in the digester would be so high, that the AD process will be already severely inhibited [39].

4.3.5. Ammonia

Ammonia (NH3) is an important nutrient, serving as a antecedent to food stuffs and fertilizers and is normally encountered as a gas, with the characteristic strong smell. Proteins are the main source of ammonia for the AD process.

Too high ammonia concentration inside the digester is considered to be responsible for process inhibition. This is common to AD of animal slurries, due to their high ammonia concentration, originating from urine. For its inhibitory effect, ammonia concentration should be kept below 80 mg/l. Methanogenic bacteria are especially sensitive to ammonia inhibition. The concentration of free ammonia is direct proportional to temperature, so there is an increased risk of ammonia inhibition of AD processes operated at thermophilic temperatures, compared to mesophilic ones. The free ammonia concentration is calculated from the equation:

$$[NH_3] = \frac{[T-NH_3]}{\left(1+\frac{H^+}{ka}\right)} \quad (4.1)$$

Where $[NH_3]$ and $[T\text{-}NH_3]$ are the free and respectively the total ammonia concentrations, and *ka* is the dissociation parameter, with values increasing with temperature. This means that increasing pH and increasing temperature will lead to increased inhibition, as these factors will increase the fraction of free ammonia. When a process is inhibited by ammonia, an increase in the concentration of VFA will lead to a decrease in pH. This will partly cancel out the effect of ammonia due to a decrease in the free ammonia concentration [36].

4.3.6. Macro- and micronutrients (trace elements) and toxic compounds

Microelements (trace elements) like iron, nickel, cobalt, selenium, molybdenum or tungsten are equally important for the growth and survival of the AD microorganisms as the macronutrients carbon, nitrogen, phosphor, and sulphur. The optimal ratio of the macronutrients carbon, nitrogen, phosphor, and sulphur (C: N: P: S) is considered 600:15:5:1. Insufficient provision of nutrients and trace elements, as well as too high digestibility of the substrate can cause inhibition and disturbances in the AD process.

Another factor, influencing the activity of anaerobic microorganisms, is the presence of toxic compounds. They can be brought into the AD system together with the feedstock or are generated during the process. The application of threshold values for toxic compounds is difficult, on one hand because these kind of materials are often bound by chemical processes and on the other hand because of the capacity of anaerobic microorganisms to adapt, within some limits, to environmental conditions, herewith to the presence of toxic compounds [36].

4.4. Operational Parameters for Biogas Plant

4.4.1. Organic Load

The construction and operation of a biogas plant is a combination of economic and technical considerations. Obtaining the maximum biogas yield, by complete digestion of the substrate, would require a long retention time of the substrate inside the digester and a correspondingly large digester size. In practice, the choice of system design (digester size and type) or of applicable retention time is always based on a compromise between getting the highest possible biogas yield and having justifiable plant economy. In this respect, the organic load is an important operational parameter, which indicates how much organic dry matter can be fed into the digester, per volume and time unit, according to the equation below [38]:

$$B_R = m * \frac{c}{V_R} \tag{4.2}$$

Where, B_R = organic load [kg/d*m³]

m = mass of substrate fed per time unit [kg/d]

c = concentration of organic matter [%]

V_R = digester volume [m³]

4.4.2. Hydraulic Retention Time (HRT)

An important parameter for dimensioning the biogas digester is the hydraulic retention time (HRT). The HRT is the average time interval when the substrate is kept inside the digester tank. HRT is correlated to the digester volume and the volume of substrate fed per time unit, according to the following equation [38]:

$$HRT = \frac{V_R}{V} \tag{4.3}$$

Where, HRT= hydraulic retention time [days]

VR = digester volume [m³]

V = volume of substrate fed per time unit [m³/d]

According to the above equation, increasing the organic load reduces the HRT. The retention time must be sufficiently long to ensure that the amount of microorganisms removed with the waste matter is not higher than the amount of reproduced microorganisms. The duplication rate of anaerobic bacteria is usually 10 days or more. A short HRT provides a good substrate flow rate, but a lower gas yield. It is therefore important to adapt the HRT to the specific decomposition rate of the used substrates. Knowing the targeted HRT, the daily feedstock input and the decomposition rate of the substrate, it is possible to calculate the necessary digester volume.

4.5. Biogas Digester Sizing

The energy available from a biogas digester is given by [19]:

$$E = \eta H_b V_b \tag{4.4}$$

where η is the combustion efficiency of burners, boilers, etc. (~60%). H_b is the heat of combustion per unit volume biogas ($20 MJm^{-3}$ at 10 cm water gauge pressure, 0.01 atmospheres) and V_b is the volume of biogas. Note that some of the heat of combustion of the methane goes to heating the CO_2 present in the biogas, and is therefore unavailable for other purposes. The net effect is to decrease the efficiency.

Alternatively:

$$E = \eta H_m f_m V_b \tag{4.5}$$

where H_m is the heat of combustion of methane ($56 MJkg^{-1}$, $28 MJm^{-3}$ at STP) and f_m is the fraction of methane in the biogas. As from the digester, f_m should be between 0.5 and 0.7, but it is not difficult to pass the gas through a counter flow of water to dissolve the CO_2 and increase f_m to nearly 1.0.

The volume of biogas is given by

$$V_b = c m_o \tag{4.6}$$

Where $\boldsymbol{c}$ is the biogas yield per unit dry mass of whole input 0.2– $0.4 m^3\ kg^{-1}$ and m_o is the mass of dry input.

The volume of fluid in the digester is given by

$$V_f = {}^{m_o}/_{\rho_m} \tag{4.7}$$

Where ρ_m is the density of dry matter in the fluid (~50 kgm^{-3}).
The volume of the digester is given by

$$V_d = \tilde{V}_f t_r \tag{4.8}$$

Where $\tilde{V}_f^{\cdot}$ is the flow rate of the digester fluid and t_r is the retention time in the digester (~8–20 days).

4.6. Technologies for Biogas Conversion into Electricity

There are different kinds of technology to convert the chemical energy in the biogas into electricity. In biogas conversion the chemical energy in the molecules is converted to mechanical energy in a controlled combustion system, then, this mechanical energy activates a generator producing electrical power. The gas turbines and the internal combustion engines are the most common technologies used to this kind of energy conversion.

In most cases, biogas is used as fuel for combustion engines, which convert it to mechanical energy, powering an electric generator to produce electricity. Appropriate electric generators are available in virtually all countries and in all sizes. The technology is well known and maintenance is simple. In theory, biogas can be used as fuel in nearly all types of combustion engines, such as gas engines (Otto motor), diesel engines, gas turbines and Stirling motors etc [41].

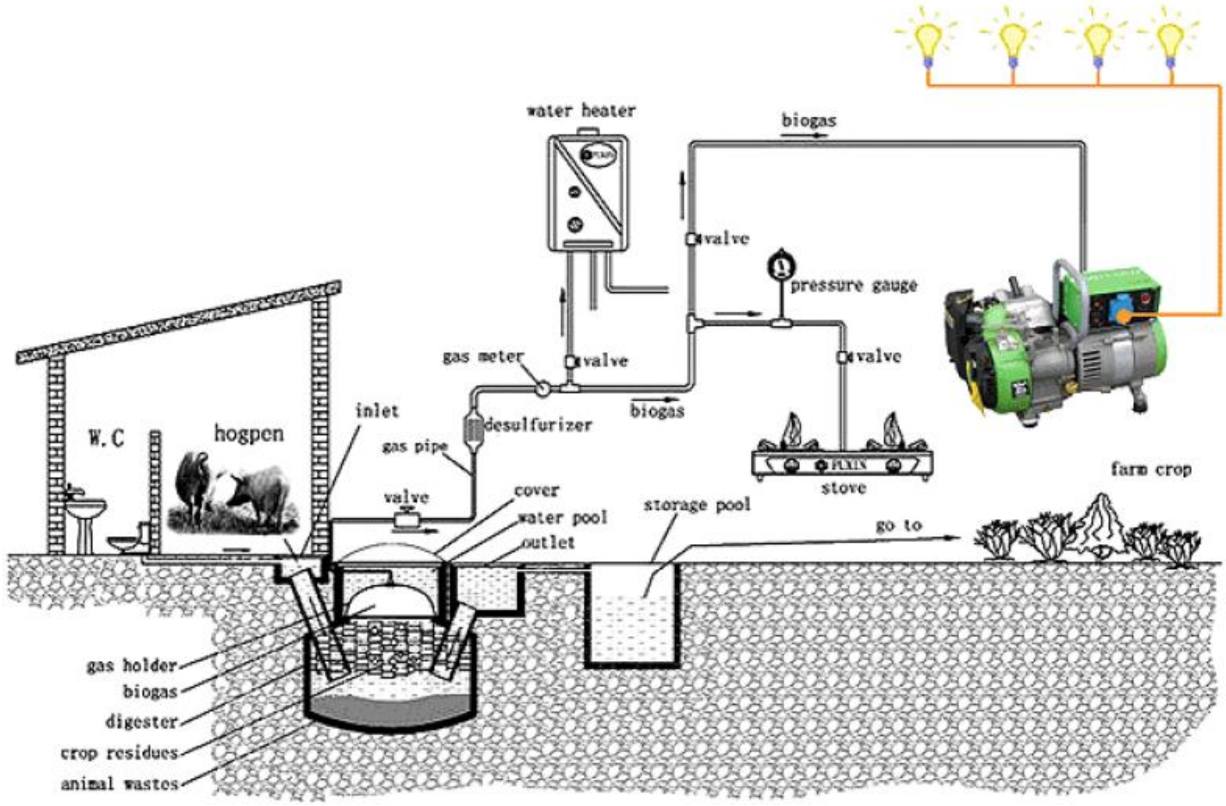

Figure 4.3: Schematic of a biogas plant used for power generation [42]

4.7. Utilizations of biogas energy

Generally, biogas can be used for heat production by direct combustion, electricity production by fuel cells or micro-turbines, CHP generation or as vehicle fuel.

- **Direct Combustion and Heat Utilization**

The simplest way of utilizing biogas is direct burning in boilers or burners, extensively used for the biogas produced by small family digesters. Biogas can be burned for heat production either on site, or transported by pipeline to the end users. For heating purposes biogas does not need any upgrading, and the contamination level does not restrict the gas utilization as much as in the case of other applications. However, biogas needs to undergo condensation and particulate removal, compression, cooling and drying [38].

- **Combined Heat and Power (CHP) Generation**

CHP generation is a standard utilization of biogas from anaerobic digestion after it has been drained and dried. Most gas engines have maximum limits for the content of hydrogen sulphide, halogenated hydrocarbons and siloxanes in biogas. An engine based CHP power plant has an efficiency of up to 90% and produces 35% electricity and 65% heat [40].

- **Biogas Micro-turbines**

In biogas micro-turbines, air is pressed into a combustion chamber at high pressure and mixed with biogas. The air-biogas mixture is burned causing the temperature increase and the expanding of the gas mixture. The hot gases are released through a turbine, which is connected to the electricity generator (Figure 4.4). The electric capacity of micro-turbines is typically below 200 kWe.

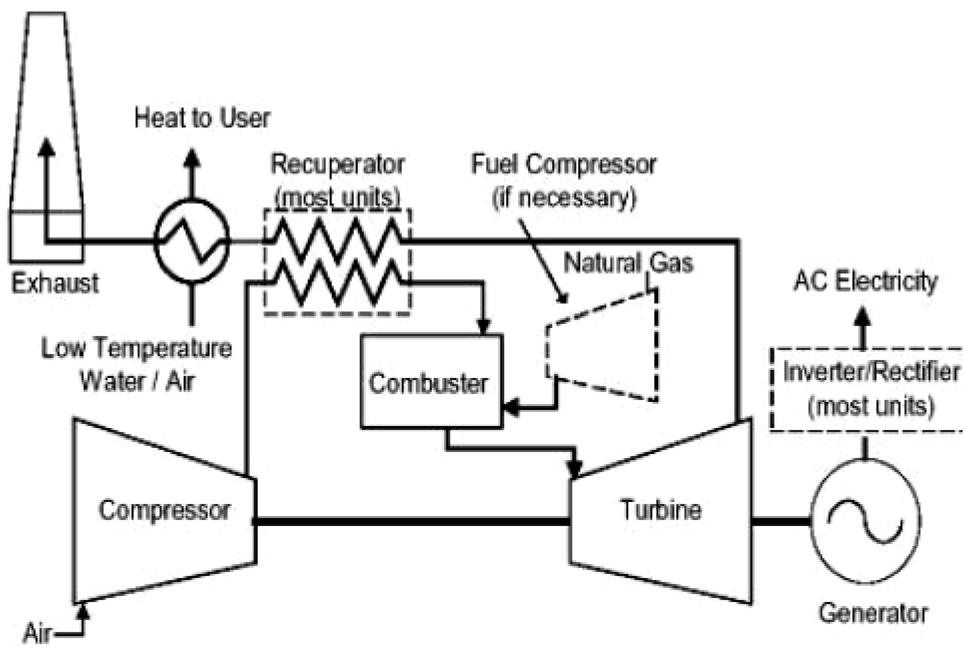

Figure 4.4: Micro-turbine structure [43]

- **Fuel cells**

The fuel cells are electrochemical devices that convert the chemical energy of a reaction directly into electrical energy. The basic physical structure (building block) of a fuel cell consists of an electrolyte layer in contact with a porous anode and cathode on both sides (Figure 4.5). In a typical fuel cell, the gaseous fuel (biogas) is fed continuously to the anode (the negative electrode) compartment and an oxidant (i.e. oxygen from air) is fed continuously to the cathode (the positive electrode) compartment. An electrochemical reaction takes place at the electrodes, producing electric current.

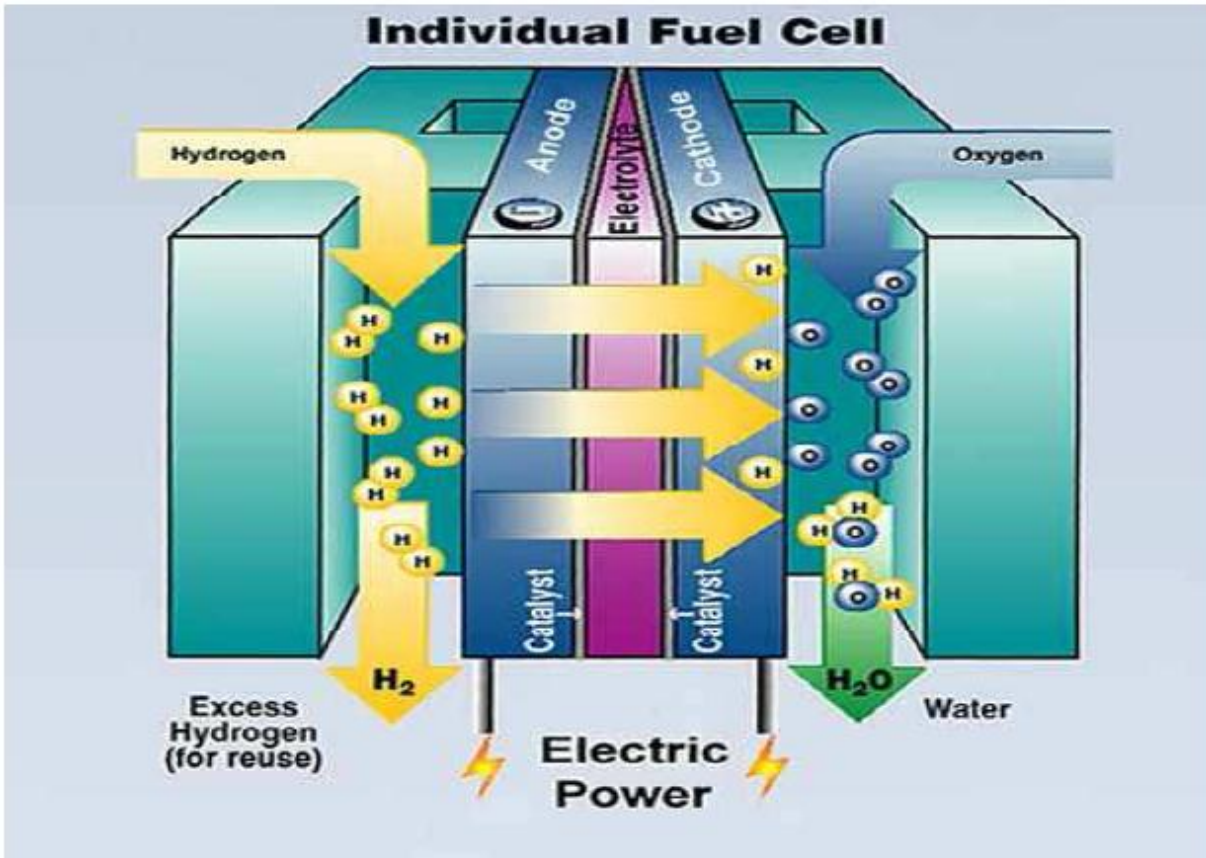

Figure 4.5: Simplified scheme of a fuel cell [38]

- **Biogas Upgrading (Biomethane Production)**

Biogas can be distributed through the existing natural gas networks and used for the same purposes as natural gas or it can be compressed and used as renewable vehicle fuel. Earlier to injection into the natural gas grid or to utilization as vehicle fuel, biogas must undergo an upgrading process, where all contaminants as well as carbon dioxide are removed and the content of methane increases from the usual 50-75% to more than 95%. The upgraded biogas is often named Biomethane. Various technologies can be applied for removal of contaminants and for increasing the methane content of biogas.

As methane has a 23-fold stronger greenhouse gas effect than CO_2, (i.e. a molecule of methane is 23 times more effective than a molecule of CO_2 in trapping the radiated heat from earth) it is important to keep methane losses low, for both economic and environmental reasons. Two common methods of removing carbon dioxide from biogas are absorption (water scrubbing, organic solvent scrubbing) and adsorption (pressure swing adsorption). Less frequently used are membrane separation, cryogenic separation and process internal upgrading, which is a relatively new method, currently under development [38].

4.8. Biogas Resource Potential in Ethiopia

Given resource potential, biogas is one of the promising clean energy for Ethiopian households. It involves gasification of biomass resources. The only technology for biogas production in Ethiopia so far is anaerobic digestion/fermentation that is based on animal residue. The major advantage of biogas based on manure is that it is renewable. Ethiopia is the first in Africa and tenth in the world in terms of livestock ownership. Biogas technology has been implemented at small scale rural and off-grid areas [44].

Dung input has competitive use as fertilizer. Cost of fertilizer has been rising. Compost obtained from biogas provides alternative fertilizer for farmers. Hence biogas has an ability to reduce burden of rising price of fertilizer. But its utilization is hindered by various factors. The prime challenge is cost of financing which poor rural households are unable to afford. Hence, collective actions and institutions for decentralized biomass fuel/biogas are crucial for channeling finance and technology to remote rural areas.

Table 4.3: Overview of technical data of the four regions of Ethiopia to be used for biogas plant construction

Region	Area (Km^2)	Households (# of hh)	Cattle holdings (# of ch)	Cattle population (# of heads)	% cattle holdings [%]	Cattle density [head /km^2]	Avg. cattle /hh
Amhara	148509	3194754	2574836	10275527	81	69	4
Oromia	328939	4564213	3594072	18575227	79	56	5.2
SNNPRs	112217	2688970	2009680	8815689	75	79	4.4
Tigray	50182	724964	559334	2665129	77	53	4.8
Total	639846	11172901	8737922	40331572	78	63	4.6

Source: Ministry of Mines and Energy (MME)

4.8.1 Biogas Resource Assessment of the Study Area

As previously discussed, in Ethiopia there are large numbers of pastoral farmers and many literatures reviewed the number of cattle for the zone level throughout the country. According to the 2010/11 agricultural sample survey by Central Statistical Agency of Ethiopia, the number of cattle in the zones of Tigray is mentioned in Table 4.4 below. Studies conducted by Ministry of Mines and Energy of Ethiopia indicate that the average daily dry mass of manure obtained per a cattle is taken as 5 kg [35].

Table 4.4: Overview of technical data of the four zones of Tigray to be used for biogas plant construction

Tigray / Zone	Area (Km^2)	Households (# of hh)	Cattle holdings (# of ch)	Cattle population (# of heads)	% cattle holdings [%]	Cattle density [head /km^2]	Avg. cattle/hh
Central Tigray	10327	230761	174810	627831	76	61	3.6
Southern Tigray	9408	183354	136515	631185	74	67	4.6
Western Tigray	24652	180952	152793	1081963	84	44	7.1
Eastern Tigray	5795	129897	95216	324150	73	56	3.4
Total	50182	724964	559334	2665129	77	53	4.8

Based on the Table 4.4 above the digester and biogas size for the site is calculated as follows.

- It is assumed that 73% of the total residents in the community own cattle. The assumption is based on the cattle density in the zone -Eastern Tigray (see Table 4.4 above).
- The average cattle holding per household is 3.4 (for Eastern Tigray).Therefore, the total number of cattle for the site having 200 households will be 200*3.4= 680.
- The average daily dry mass of manure obtained per cattle is taken as 5 kg and the total daily mass for the site having 200 households is 5*680=3400kg/day or 3.4 tonnes/day. Therefore, the monthly average cattle's manure obtained from the site for each month is calculated and given in Table 4.5 below. This value is used as an input to the software for modeling the biogas energy potential.
- The digester volume, Vd, is determined from the volume of fluid in the digester (V_f) and hydraulic retention time (HRT) using the above mentioned equations namely 4.3&4.9. The volume of the fluid in the digester is calculated using the mass of dry input (m) and

the density of dry matter in the fluid (gm) which is taken as 50kgm^{-3}. Hydraulic retention time that can be used is 20 days and retention time larger than these days is uneconomical [19].

- The volume of the biogas is calculated from the dry mass input and from the biogas yield for unit dry mass of the whole input (C). A biogas yield from cattle dung is 0.2-0.4 m^3/kg [19].

Table 4.5: Monthly average cattle's manure (tonnes/day) at the site

Month	J	F	M	A	Ma	Ju	Jul	Au	S	O	N	D
Cattle manure (tonnes/ day)	105.4	95.2	105.4	102	105.4	102	105.4	105.4	102	105.4	102	105.4

CHAPTER FIVE

HYBRID SYSTEM OPTIMIZATION USING HOMER AND COST OF GRID EXTENSION

Hybrid energy system is an excellent solution for electrification of remote rural areas where the grid extension is difficult and not economical. Such system incorporates a combination of one or several renewable energy sources such as solar photovoltaic, biogas energy, wind energy and battery. A hybrid system uses a combination of energy producing components that provide a constant flow of uninterrupted power.

Other advantages of the hybrid system are the stability and immobility of the system and a lower maintenance requirement, thus reducing downtime during repairs or everyday maintenance. In addition to this, as well as being indigenous and free, renewable energy resources also contribute to the reduction of emissions and pollution [30].

5.1. Modeling of Hybrid System with HOMER

HOMER is a user-friendly micro-power design tool that was developed by NREL in the U.S.A to assist the design of power systems and facilitate the comparison of power generation technologies across a wide range of applications [45]. HOMER is used to model a power system physical behavior and its life-cycle cost, which is the total cost of installing and operating the system over its life time. HOMER allows the modeler to compare many different design options based on their technical and economic merits. It also assists in understanding and quantifying the effects of uncertainty or changes in the inputs. HOMER was designed to overcome this uncertainty and also the complexity of the renewable energies being intermittent, seasonal, non-dispatchable and having uncertain availability.

The design of a stand-alone PV-wind-biogas hybrid energy system to a model community of 200 households, with average six members per family was carried out based on the theoretical background discussed so far. HOMER software is used as a tool to accomplish the research. As earlier, the main objective of the study is to design and model hybrid PV–Wind–biogas–battery based standalone power generation systems to meet the load requirements of the community specified earlier. A schematic representation of the standalone hybrid energy system by HOMER is shown in Figure 5.1.

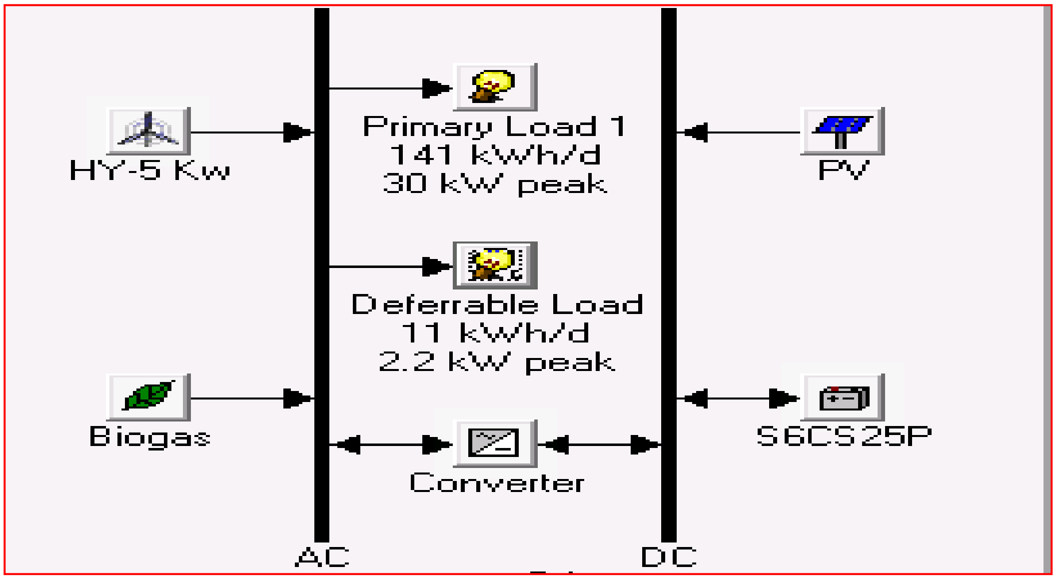

Figure 5.1: HOMER diagram for the hybrid PV-wind-biogas-battery-converter set-up

HOMER performs three principal tasks: simulation, optimization, and sensitivity analysis. In the simulation process, the performance of a particular power system configuration for each hour of the year is modeled to determine its technical feasibility and life-cycle cost. In the optimization process, many different system configurations are simulated in search of the one that satisfies the technical constraints at the lowest life-cycle cost. In the sensitivity analysis process, multiple optimizations are performed under a range of input assumptions to judge the effects of uncertainty or changes in the model inputs. Optimization determines the optimal value of the variables over which the system designer has control such as the mix of components that make up the system and the size or quantity of each. Sensitivity analysis helps assess the effects of uncertainty or changes in the variables over which the designer has no control, such as the average wind speed or the future fuel price. The effects of these can be analyzed with the help of the sensitivity analysis.

Figure 5.2 shows how simulation, optimization and sensitivity analysis are interrelated. The oval figure enclosed in another oval figure shows that one optimization consists of multiple simulation and one sensitivity analysis consists of multiple optimizations.

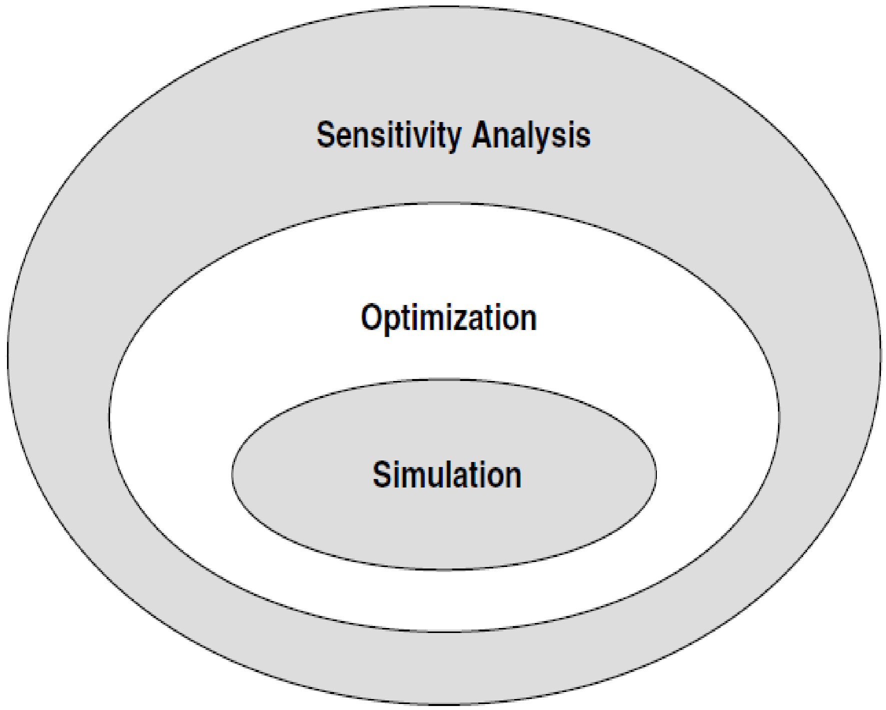

Figure 5.2: Conceptual relationship between simulation, optimization, and sensitivity analysis.

In the next section how HOMER models the physical operation of a system is provided in greater detail. A power system must comprise at least one source of electrical energy (such as SPV system, a biogas generator, a wind turbine, or the grid), and at least one destination for that energy (electrical load). It may also comprise conversion devices such as a dc-ac converter or an electrolyzer, and energy storage devices such as a battery bank or a hydrogen storage tank.

The following subsections are devoted on how to model the loads that the system must serve, the components of the system and their associated resources, and how that collection of components operate together to serve the loads.

5.2. Electric Load Estimation and Forecasting

5.2.1. Electric Load Estimation

One of the basic inputs to HOMER is the load profile of the system. The term loads refers to a demand for electric energy. Two types of loads can be modeled using HOMER: primary load which is electric demand that must be served according to a particular schedule, deferrable load which is electric demand that can be served at certain period of time, the exact timing is not important.

According to Bekele G. [30], electric load in the rural villages of Ethiopia can be assumed to be composed of lighting, radio and television, water pumps, health post and primary schools load. Tamrat B. [10] considered only lighting, radio and television as a community load. In this study, electricity for flour mills is added to the load together with radio receiver and health post is upgraded to health clinic with additional medical equipment. Water pumps are considered as deferrable loads while the others as primary loads. As introduced earlier, the community understudy, which equipped with primary school and a health clinic, has 200 households with an average 6 members per family.

For the community a flour mill of 12.5 kW working from 9:00 to 11:00 and 15:00 to 18:00 are assumed. Each household is to be installed with 3 CFLs of 11W rating to be lit from 18:00 to 23:00. Additionally a CFL of 11W is also considered for external lighting. A radio receiver (5W) and a TV set (70W) are to be used in the time 18:00 to 23:00.

Primary school consists of 15 classrooms and each classroom will be installed with four 11W CFLs (compact fluorescent lamps) and a 5W radio receiver. An 11 W CFL has an equivalent lumens effect of a 60 W incandescent lamp. Additional 6 CFLs (of 11W) for external lighting and five 11W lamp for a toilet are also considered. Evening classes are conducted from 18:00 to 21:00 and the receivers are used for radio lessons. Similarly for the health clinic, having 5 rooms, one 11W CFL per room and two 11W CFL for external lighting are considered. A vaccine refrigerator of 80W working for 24 hours; a 20W capacity microscope and a 5 W radio receiver for the office hours; and a 1 kW water heater operational for 3 hours per day are also suggested for health clinic. One ceiling fan (75W) per room is also to be installed for air conditioning purpose between 10:00 and 15:00.

Water pumping system is required for the households, the school and health clinic. A minimum of 100 l of water per day per family and 2400 l/day for health clinic and primary school is suggested [6, 30]. To accomplish this, 3 water pumps of 270 W(with a nominal flow rate of 1.21 m^3/hr , nominal head of 30 m and efficiency of 36.5%) operating for 6 hours/day are to be installed to supply water for the community. Another 1 pumps of 270 W (with a nominal flow rate of 1.21 m^3/hr, nominal head of 30 m and a capacity of 40 l/m) for the public services operating for 2 hours/day are assumed. A water storage capacity of 3 days is suggested requiring a storage capacity of 14.58 kWh for the community and 1.62 kWh for public centers. The peak deferrable load is 0.81 kW for community and 0.27 kW for the public centers.

Exceptions: In the weekends it is assumed that flour mills are not working because of religious concern and evening classes are conducted at day time. In the rainy season from 15% to 30% deferrable load can be expected to decrease because water consumption from the pumps is expected to be shared by river and rain water ponds [6]. 15% deferrable load decrease for June and September while 30% for July and August are assumed. There are no classes in July and August (annual break) and in January (semester break).

Table 5.1: Monthly average daily electrical energy consumption (kWh)

Months	Jan	Feb-May	June	Jul & Aug	Sep	Oct-Dec
Deferrable Load	11.8	11.8	10.1	7.722	10.1	11.8
Primary Load	141.4	143.9	143.9	141.4	143.9	143.9
Total Load	153.2	155.7	154	149.12	154	155.7

The 24 hour primary and deferrable load profiles are given in Figures 5.3 and 5.4 respectively.

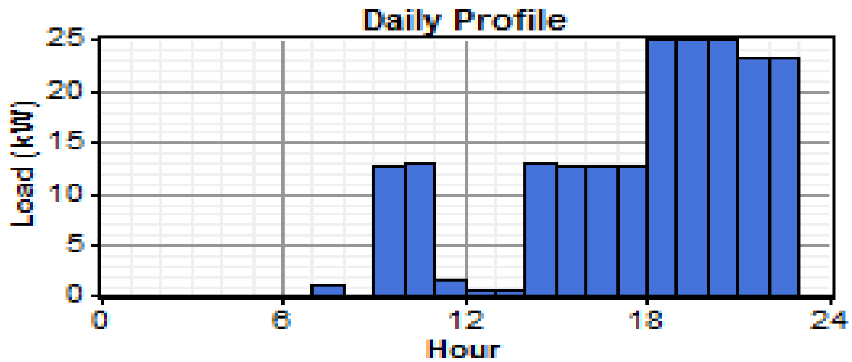

Figure 5.3: Primary load profile of the community

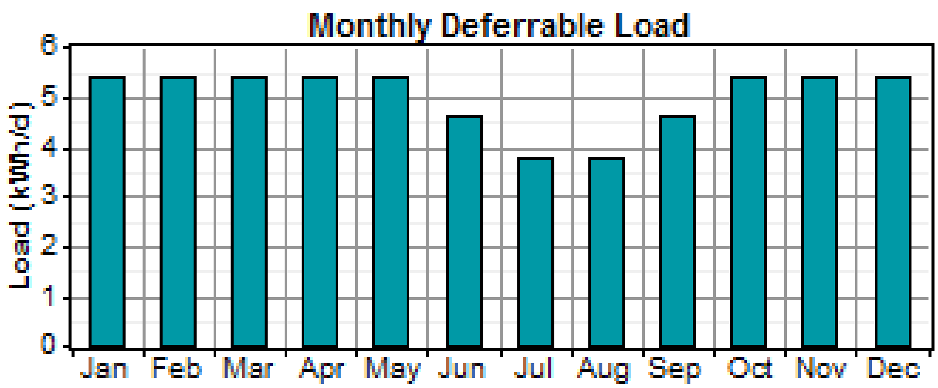

Figure 5.4: Monthly average deferrable load profiles.

5.2.2. Electric Load Forecasting of the Study Area

A forecast of electricity demand of the village is made based on a method known as energy approach. In this approach the annual energy for residential customers are forecasted using appropriate growth rates such as population growth rates, customer growth (market penetration) and growth rates of consumption per connection which are described in the sections below [15,46].

- **Population Growth Rate**

First year population figure is projected by an annual growth rate of 3%, until the end of the forecast period. This population figure is converted to total number of households using an assumed average number of occupants per household [15, 46].

- **Residential Consumption**

The number of potential residential customers is changed to annual residential consumption by assuming an average per household consumption, which starts with 304 kWh on the first year. This average consumption per household is made to grow at a rate of 2.57% per year for the whole forecast period [15, 46].

- **Market Penetration(Customer Growth)**

At the first year of electrification, all households are assumed to be connected. Therefore, market penetration rate is necessary. After the first year of interconnection, 5% market penetration rate (MP) is taken to change the total number of households to potential residential customers until the end of forecast [15,46].

Table 5.2: Energy forecast for the study area

Year	No. Household	Yearly energy consumption(KWh)	Daily energy consumption(KWh)
2013	200	60,800	166.6
2014	210	65,478	179.4
2015	222	70,995.6	194.5
2016	233	76,424	209.38
2017	245	82,425.35	225.82
2018	257	88,665	242.92
2019	270	95,580	261.86
2020	284	103,092	282.44
2021	298	110,856	303.72
2022	313	119,440.8	327.24
2023	329	128,770.6	352.8
2024	346	138,919	380.60
2025	363	149,556	409.74
2026	381	161,010.6	441.12
2027	400	173,400	475.07
2028	420	186,690	511.48
2029	441	201,096	575.61
2030	463	216,684	539.65

2031	486	233,280	639
2032	510	250,920	687.5
2033	536	270,680	742

The above Table shows the forecasted yearly and daily energy consumption of the community for 20 years using energy approach method. This method is employed as the HOMER software used in this thesis doesn't take in to account the forthcoming variation of energy consumption of the community. This is taken as a fundamental draw back or limitation of the software.

5.3. Resource Assessment

The term resource applies to anything coming from outside the system that is used by the system to generate electric power. That includes the four renewable resources (solar, wind, hydro, and biogas) as well as any fuel used by the components of the system. Renewable resources depend extremely on location. The solar resource depends strongly on latitude and climate, the wind resource on large-scale atmospheric circulation patterns and geographic influences, the hydro resource on local rainfall patterns and topography, and the biomass resource on local biological productivity. Moreover, at any one location a renewable resource may exhibit strong seasonal and hour-to-hour variability. The nature of the available renewable resources affects the behavior and economics of renewable power systems, since the resource determines the quantity and the timing of renewable power production. The careful modeling of the renewable resources is therefore an essential element of system modeling. In this section how to model the renewable resources used in this thesis is described [47, 48].

***Solar Resource*:** To model a system containing a PV array, the solar resource data for the location of interest has been provided. Solar resource data indicate the amount of global solar radiation (beam radiation coming directly from the sun, plus diffuse radiation coming from all parts of the sky) that strikes Earth's surface in a typical year. The data can be in one of three forms: hourly average global solar radiation on the horizontal surface (kWh/m^2), monthly average global solar radiation on the horizontal surface (kWh/m^2.day), or monthly average clearness index. The clearness index is the ratio of the solar radiation striking Earth's surface to the solar radiation striking the top of the atmosphere. A number between zero and one, the clearness index is a measure of the clearness of the atmosphere.

The solar radiation data of the site was fed into HOMER and this is depicted in Figure 5.5. This figure also shows the clearness index, the ratio of the solar radiation striking Earth's surface to the solar radiation striking the top of the atmosphere, which HOMER generated from global solar radiation for the analysis. Typical values for the monthly average clearness index range from 0.539 (a cloudy month) to 0.725 (a very sunny month).

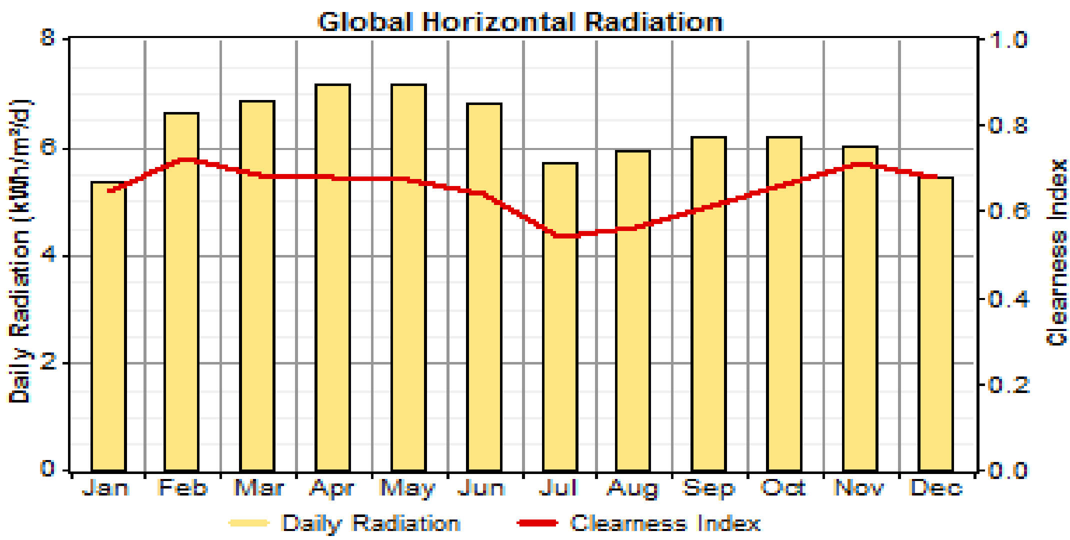

Figure 5.5: Monthly average solar radiation

Wind Energy Resource**:** To model a system comprising one or more wind turbines, the wind resource data indicating the wind speeds the turbines would experience in a typical year has been provided. The user can provide measured hourly wind speed data if available. Otherwise, HOMER can generate synthetic hourly data from 12 monthly average wind speeds and four additional statistical parameters: the Weibull shape factor, the autocorrelation factor, the diurnal pattern strength, and the hour of peak wind speed.

The Weibull shape factor is a measure of the distribution of wind speeds over the year. The autocorrelation factor is a measure of how strongly the wind speed in one hour tends to depend on the wind speed in the preceding hour [45]. For complex topography the autocorrelation factor is (0.70 - 0.80) while for a uniform topography the range is higher, (0.90 - 0.97). A typical range for the autocorrelation factor is 0.8 – 0.95 [45]. An average value of 0.85 is used here because the selected areas are of averagely uniform topography. The diurnal pattern strength is a measure of how strongly the wind speed tends to depend on the time of day [45]. Typical values for diurnal pattern strength range from 0 to 0.4. A value of 0.25 has been selected for calculations. The hour of peak wind speed is the hour of the day that tends, on average, to be the windiest throughout the year. The typical range for the time of peak wind speed is 14:00-16:00 [45]. This has also been observed in the available raw data for some of the months. In addition to this, the software has been run for different times between 14:00 and 18:00, the results have been checked against the measured data and the time of 15:00 has been chosen for the calculations.

The anemometer height, which is the height above ground at which the wind speed data were measured, has been defined. The elevation of the site above sea level, which is used to calculate the air density according to equations 3.7-3.8, is also defined.

The monthly average wind speed for site, together with other related data, such as values of Weibull parameter k, diurnal pattern, autocorrelation, etc, was fed into HOMER. Figure 5.6 shows the wind speed resource data measured at 10 m height.

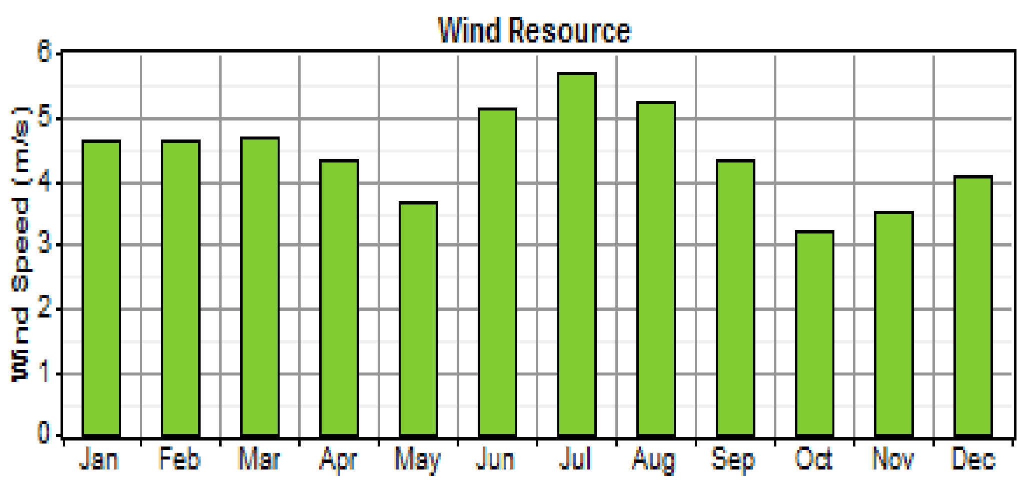

Figure 5.6: Monthly average wind speed at 10 m

Biogas Energy Resource**:** The physical properties of a biogas fuel include its gasification ratio, lower heating value, carbon content and the average price. The user can also choose the most appropriate measurement units, L, m^3, or kg.

Gasification ratio is the mass of biogas produced per unit mass of feedstock consumed. Lower heating value is the heat content of biogas. The carbon content is the net amount carbon released per unit of feedstock consumed. The average price per tonnes of the biogas feedstock is taken 12 $ [35].

The monthly average biogas feedstock(cattle's manure) of the site, together with other related data, such as values of gasification ratio, carbon content, autocorrelation, average price per tonnes of the biogas feedstock, lower heating value etc, was fed into HOMER. Figure 5.7 shows the biogas feedstock resource.

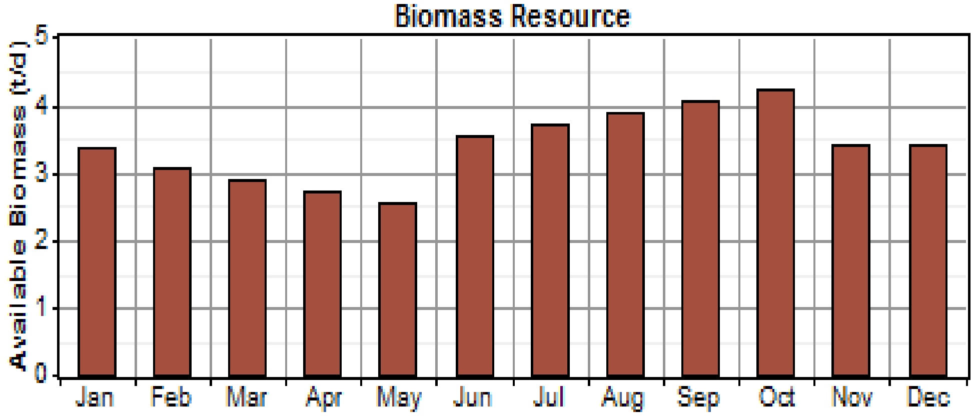

Figure 5.7: Monthly average biogas feedstock (cattle's manure)

5.4. Components Assessment

A component is any part of a power system that either generates, delivers, converts, or stores energy. In this HOMER analysis the basic components of the hybrid system are SPV, wind turbines, and biogas generator. Others are additional/auxiliary components which help for full time functioning of the hybrid system such as Batteries and Converters. Batteries and Converters are for storing and converting electricity respectively. The Grid connection in this study is only used as a comparison for the analysis and determination of the break even distance. The performance and cost of each of the system’s components is a major factor for the cost results and the design. Thus, the development of these data was carried out with much diligence. A different set of performance and cost parameters is used by HOMER to characterize each of these different components. The principle of operation of the basic components has been covered.

Solar Array: The PV array is a device that produces dc electricity in direct proportion to the global solar radiation incident upon it. In this paper, the derating factor considered is 90% for each panel to approximate the varying affects of temperature and dust on the panels. The panels have no tracking system and are modeled as fixed latitude of the location with the slope of 14°.

To describe the cost of the PV array, its initial capital cost in dollars, replacement cost in dollars, and operating and maintenance (O&M) cost in dollars per year has been specified in Table 5.3 below taken from different sources [49,50]. The replacement cost is the cost of replacing the PV array at the end of its useful lifetime, which is specified in years. By default, the replacement cost is equal to the capital cost.

Wind turbine**:** A wind turbine is a device that converts the kinetic energy of the wind into ac or dc electricity according to a particular power curve, which is a graph of power output versus wind speed at hub height.

Each hour, the power output of the wind turbine is calculated in a four-step process. First, the average wind speed for the hour at the anemometer height is determined by referring to the wind resource data. Second, the corresponding wind speed at the turbine's hub height is calculated using either the logarithmic law or power law. Third, the power output of wind turbine is calculated at that wind speed referring to its power curve assuming standard air density. Fourth, that power output value is multiplied by the air density ratio, which is the ratio of the actual air density to the standard air density.

In addition to the turbine's power curve and hub height, the expected lifetime of the turbine in years, its initial capital cost in dollars, its replacement cost in dollars, and its annual O&M cost in dollars per year has been specified.

The primary criterion for the selection of the wind turbine is its cost. The wind turbines have been selected from different sources; the various wind turbine websites and those suggested by the HOMER program itself based on their costs. Other selection criteria used are: the type of current they generate (ac or dc), how low the cut-in wind speed is, and for what application the wind turbine be used for. The cut-in wind speed is another is primary criterion, if not import than cost, as the wind resource at the site is not very high. The type of current they generate, whether ac or dc, is also considered as it have impacts on the size of the inverter. As the load assumed for the households is of an ac type a wind turbine that generates ac current has been chosen. As the aim of the research is to supply electric energy to remotely located communities, the wind turbines selected should be those which are applicable for home or off grid applications.

Based on the selection criteria mentioned above, the HY-5 type has been found to be the best in terms of the cut-in wind speed and also in respect to other criteria mentioned earlier. This was obtained from those wind turbine website (www.huayingwindpower.com) owned by Hulk Energy Machinery [51, 52].

Biogas Generator**:** A biogas generator consumes fuel (biogas) to produce electricity, and possibly heat as a byproduct. The generator module is flexible enough to model a wide variety of generators, including internal combustion engine generators, micro-turbines, fuel cells, etc.

The principal physical properties of the biogas generator are its maximum and minimum electrical power output, its expected lifetime in operating hours, the type of fuel it consumes, and its fuel curve, which relates the quantity of fuel consumed to the electrical power produced. In addition to these properties, the biogas generator emissions coefficients, which specify the generator's emissions of six different pollutants in grams of pollutant emitted per quantity of fuel consumed can be specified.

The generator's initial capital cost in dollars, replacement cost in dollars, and annual O&M cost in dollars per operating hour taken from different sources has been specified [53]. 70% of a minimum load ratio, an intercept coefficient of 0.0025/hr/kW and slope of 0.852 kg/hr/kW are taken for generator [54]. The biogas generator efficiency against its percentage loading is given in Figure 5.8 below.

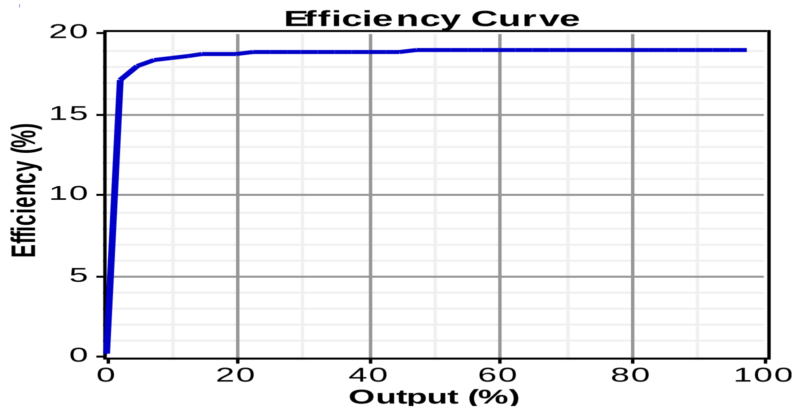

Figure 5.8: Biogas generator efficiency curve

***Battery*:** A battery is a device capable of storing a certain amount of DC electricity at fixed round-trip energy efficiency, with limits as to how quickly it can be charged or discharged, how deeply it can be discharged without causing damage, and how much energy can cycle through it before it needs replacement.

The key physical properties of the battery are its nominal voltage, capacity curve, lifetime curve, minimum state of charge, and round-trip efficiency. The capacity curve shows the discharge capacity of the battery in ampere-hours versus the discharge current in amperes. Capacity typically decreases with increasing discharge current. The lifetime curve shows the number of discharge–charge cycles the battery can withstand versus the cycle depth. The number of cycles to failure typically decreases with increasing cycle depth. The minimum state of charge is the state of charge below which the battery must not be discharged to avoid permanent damage. The round trip efficiency indicates the percentage of the energy going into the battery that can be drawn back out.

The battery bank's capital and replacement costs in dollars, and the O&M cost in dollars per year have been specified.

Converter: A converter is an electronic power device that is required in a hybrid system to maintain the energy flow between AC and DC electrical components. It has an inverter and a rectifier to do the conversions from DC to AC and vice versa. The converter size, which is a decision variable, refers to the inverter capacity, meaning the maximum amount of ac power that the device can produce by inverting dc power. The rectifier capacity, which is the maximum amount of dc power that the device can produce by rectifying ac power, as a percentage of the inverter capacity has been specified.

The final physical properties of the converter are its inversion and rectification efficiencies, which are assumed to be constant. The economic properties of the converter are its capital and replacement cost in dollars, its annual O&M cost in dollars per year, and its expected lifetime in years.

Other additional inputs into the software, such as the range of sizes for the PV, wind turbines, biogas generator and the converter and the number of batteries, are given in Table 5.3 below so as to give flexibility to the software and optimize the output results.

Table 5.3: Inputs to the HOMER software

	PV Module	Wind Turbine	Biogas Generator	Battery(6CS25P)	Converter
Size (KW)	1	5	25	1,156 Ah	1
Capital ($)	2000	4900	12,500	833	700
Replacement costs ($)	2000	3327	10,000	555	700
O&M cost ($/yr)	0	100	0.5 $/hr	15	0
Sizes Considered (KW)	0,5,10,20,30,40,50,60,70,80,100,120,150,200	________	0,10,20,30,40,50,60,70,80	____________	0,20,30,40,50,60, 80,100
Quantities considered	____________	0,5,10,15, 20,25,30,35,40,50,60	__________	0,20,30,50,70,80,90,150,200	_______
Life Time	20 yrs	20 yrs	40,000 hrs	9,645 KWh	15 yrs

5.5. Sensitivity Inputs

The key variables for the micro power system are, however, often uncertain. This is a major problem to be overcome in the designing of the system. Here, one of the most important characteristics of HOMER comes into play: This software is able to conduct a sensitivity analysis on hourly data sets with the help of scaling variables. This way, uncertainties in the primary electric load or the renewable energies (wind, hydro, solar and biogas) can be taken into account. Consequently, the sensitivity analysis allows the system designer to create a good and practical design in spite of uncertainties in the key variables [47,48].

The uncertain variables for which a sensitivity analysis had to be conducted are the wind speed and the PV capital cost multiplier inter linked with the PV replacement cost multiplier. The sensitivities entered for the PV capital cost and replacement cost are 0.4, 0.6, 0.8, and 1. For wind speed 3.5m/s, 4.42m/s and 6.0m/s are the three values entered. For each of these different values the complete system is simulated with the resulting different technical and cost parameters.

5.6. System Dispatch

Apart from choosing the different components, HOMER has to make various decisions regarding the working together of these components, such as whether power should be sold to or bought from the grid, whether batteries should be charged or discharged, which generators should operate and at what power level etc. Furthermore, all of these decisions have to be taken for every hour of the day. The concepts of operating reserve and load priority affect HOMER's dispatch decisions and are briefly discussed in the sections below [47,48].

Operating Reserve**:** Problems arising with micro power systems are the variability of the RES' power output and the possibility that the electric load demand might suddenly increase to exceed the operating capacity (which will lead to an outage). Therefore, every system needs an operating reserve, which is surplus generating capacity to provide a safety gap and be able to respond to these problems. The amount of a system's operating reserve always equals its operating capacity minus the electrical load.

***Load Priority*:** HOMER follows a load priority system, where it takes a separate set of decisions on the allocation of electricity produced by the system. HOMER serves the electricity produced from an AC source to an AC load first, the same goes for DC. In this study, as all loads are of AC connections, HOMER serves primary load followed by the deferred load.

5.7. Economic Modeling

The aim of this thesis is in finding the optimal system configuration; economics play a crucial role in the simulation. The indicator chosen to compare the different configurations' economic is the total NPC is taken as the economic figure of merit. The advantages of these indicators are described in this section.

The main difference between renewable and non-renewable resources regarding costs is that non-renewable resources usually have low capital and high operating costs, whereas for RES the costs are generally distributed in the opposite way: After a considerable investment in the beginning, the system can be operated at a comparatively low cost. To be able to compare the economics of numerous different system configurations with a varying share of renewable and non-renewable energy sources, HOMER has to take into account both the operating and capital costs. Since the NPC comprises of all costs incurred during the system's life span, it considers these factors and therefore is the appropriate parameter to compare the different configurations' economics [48].

The different items making up the NPC are the costs for construction, maintenance including component replacements and miscellaneous other costs. Furthermore, the NPC also considers salvage costs, which is the residual value of system components after the project's end [55].

An alternative to the NPC to compare the economics of various system configurations is the levelized COE, which is defined as the average cost for every kWh of electricity produced by the system. Yet, HOMER has chosen the NPC as primary economic figure of merit [55].

5.7.1. Economic inputs

The project's lifetime is considered to be 20 years with an annual interest rate of 6%. The nominal interest rate minus the inflation rate gives the real interest rate. The system fixed capital cost is considered to be $10,000 for the whole project and the system fixed O&M cost is estimated to be $500/year for the project lifetime [56]. The system fixed capital costs includes various civil constructions, logistics, labour wages, required licenses, administration and government approvals and other miscellaneous costs. The penalty for capacity shortage is not considered in this case.

5.7.2. The Grid

The grid is modeled as a component from which the micro power system either buys AC electricity or sells AC electricity by feeding it back into the grid. In this study the grid is used by HOMER, to be compared with cost of the hybrid energy system. Therefore the cost of a grid extension is taken in the analysis to see whether a grid extension is viable or it is more economical for an off-grid system to operate. This way, the breakeven grid extension distance is determined. The ***breakeven grid extension distance*** is the distance from the grid which makes the net present cost of extending the grid equal to the net present cost of the stand-alone system. Farther away from the grid, the stand-alone system is optimal. Nearer to the grid, grid extension is optimal. Figure 5.9 shows the parameters considered in this simulation by HOMER. The capital cost of grid extension per kilometer of the Midrwa village is considered to be $8021/km. The annual O&M cost per kilometer is considered to be $160.42/year/km and the grid power price is assumed from an interpolation as $0.035/kWh. The detail analysis for the cost of grid extension is briefly discussed in the section 5.8 below.

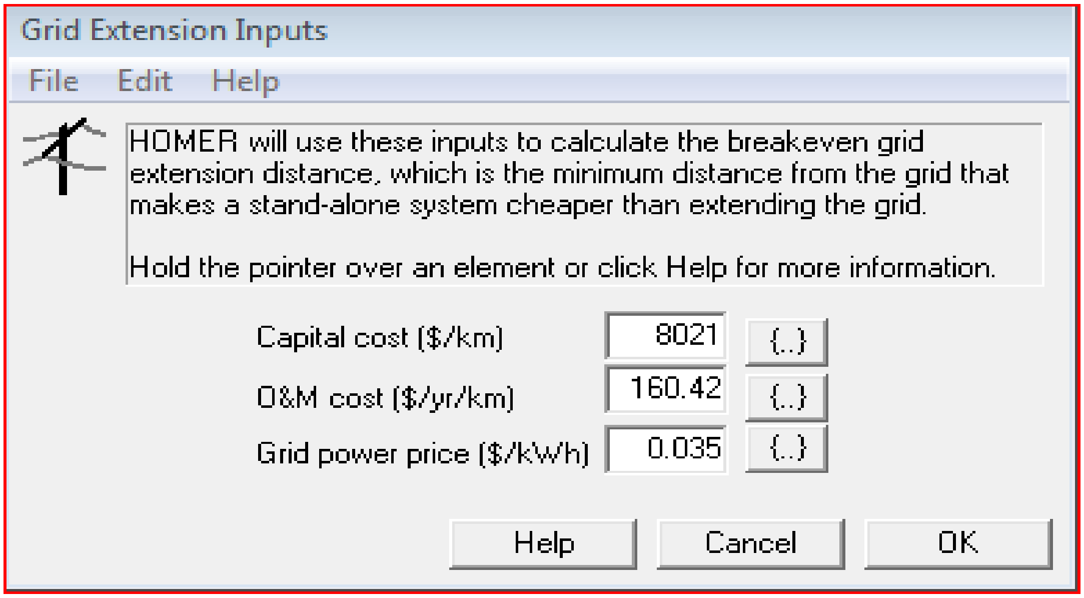

Figure 5.9: Inputs parameters of the Grid for the analysis of breakeven grid extension distance.

5.7.3. System Constraints

If a small amount of load is allowed to go unserved, this can significantly affects the economic performance of the hybrid energy system. If the system can be designed to be down for a short period of time in a year or if some load can be shed, this can help in reducing the battery bank and hence significantly reduce the capital cost of the hybrid system [57]. The maximum annual capacity shortage is set at 1% and the minimum renewable fraction is taken as 50%. It also includes the Operating reserve, which was discussed above. An operating reserve of 10% of hourly load, 25% of solar output power and 50 % wind power output respectively is suggested.

5.7.4 System Controls

There are two different types of control strategies. With the Load-following strategy, the generator is only allowed to generate power to meet the load at a given time. In contrast to this, in the Cycle charging strategy the generator is allowed to operate up to maximum power to charge the batteries and serve the load at the same time. In this study, both the strategies have been selected to see which is more suitable in the given constraints of the system. The set point charge for the batteries is kept at 80%.

5.8. Cost Estimation of Grid Extension

Power is transmitted to the end users through distribution lines. This is mainly done by extending the national grid from a near-by substation or from an over head medium voltage (MV) distribution line. The medium voltage levels that are most commonly used in MV system by the UEAP under the EEPCo are 33KV, 19KV and 15KV. But now, the UEAP is using the 33KV voltage level for electrifying the remote rural areas due to its advantage over the other options.

The main components of an overhead distribution line that can affect the cost of grid extension are: the transformer, line supports and their foundation, insulators, line accessories, conductors and overhead earth wires.

The line supports can be made from wood (like local wood pole and South Africa pole), reinforced concrete pole and steel, but due to its strength and availability UEAP is using concrete poles for MV distribution line to give electric access for selected rural areas.

The main tasks done during extension are surveying, excavation, pole erection, pole top configuration and stringing of conductors. For the MV distribution line construction Aluminum Alloy Conductor with a size of $95mm^2$ is used for the 33 KV line. However, the number of poles to be erected and the requirement of guy wire depends on the distance of the site from a nearby substation or MV distribution line, and geographical location of the selected sites. Moreover, different accessories are used depending on type of assemblies; and these can be classified as suspension, light angle 1, light angle 2, heavy angle, T-off, tension tower, and dead-end assemblies based on the angle deviation from a straight line.

Based on the data mentioned above, the cost estimation for delivering electric access to Midrwa village, which is found in Adigrat district, is done. The distance of Midrwa from an existing grid is 30km, and a rough survey is conducted to select the type of assemblies to be used for MV distribution line construction. This village needs 1x50KVA rating transformers for supplying power to the people.

To give electric access to the 200 household from the national grid found nearby, it needs extension of 30 km MV, 3.35 km LV distribution line and erection of one transformer with a rating of 50KVA. Hence, the cost is analyzed using an interlinked spread Microsoft excel sheet used by the UEAP; and the result obtained is as indicated in Table 5.4. The total cost as indicated on the table includes material, transportation and labor cost, and the investment cost is therefore **5,374,089.354 Ethiopian birr** which is equivalent to **268,704.5 US dollar**.

Table 5.4: Total cost needed for extending a grid to the site found in Adigrat district

DESCRIPTION	SALARY AND WAGE	ALLOWANCE	TRANSPORT	MATERIAL	TOTAL
33KV MV LINE EXTENSION	450,225.42	666,769.08	329,777.20	2,582,182.85	4,028,954.55
1 X200KVA ERECTION	2,350.30	3,466.86	3,252.32	45,301.52	54,371
1 X LOAD BREAK SWITCH	1,348.80	1,569.94	1020.08	16,592.56	20,531.38
LV LINE EXTENSION	79,875.40	102,224.26	88,756.55	510,822.80	781,679.01
TOTAL	**533,799.92**	**774,030.14**	**422,806.15**	**3,192,119.90**	**4,885,535.94**
	INTEREST TO BE CAPITALIZED				
	OVER HEAD COST (10%)				488,553.594
	TOTAL COST				**5,374,089.534**
	RECHARGABLE/RECOVERABLE AMOUNT (**Contributions*)				
	NET TOTAL				**5,374,089.354**

CHAPTER SIX

RESULTS AND CONCULUSIONS

In this chapter the results of the feasibility of a PV-wind-biogas hybrid power system are presented, the conclusions from the findings are drawn and at the end the recommendations are made. The feasibility of hybrid system, which supplies electricity to 200 model communities, was introduced previously. The results and conclusions of the study will be presented in the following paragraphs.

6.1. Simulation Result and Discussion

HOMER software is used for simulating the hybrid system containing PV-Wind-Biogas and storage battery as a backup. To get optimal combination of the hybrid components which could be implemented as a hybrid system model, the simulation model was run repeatedly by varying parameters that have a controlling effect over the output. These parameters are given in Table 5.3. Besides, variable of wind speed and prices of PV modules have been used for sensitivity analysis.

The software displays the result for the inputs in either an overall form in which the top ranked system configurations are listed according to their net present cost(NPC) or in categorized form in which only the most cost effective configuration is considered from each system type. Table 6.1 shows the resulting list of feasible combinations of system components in the overall form. Since the list for the overall result is long, part of it has been truncated keeping only those of greatest interest. The complete table is given in the Appendix (Table A-1). From the simulation result, different optimum and feasible system configurations with different level of total NPC are obtained. From Table 6.1, the levelized COE ranges from $0.268/kWh to $0.289/kWh.

The current energy tariff of Ethiopia is below $0.04/kWh. A previous study of Wind/PV hybrid system in Ethiopia (without biogas resource) has suggested an optimal system with a levelized COE of $0.3/kWh to $0.4/kWh [6,30]. Global electricity tariff varies in a wide range. For instance, Canada has an energy tariff of $0.0618/kWh while Denmark has $0.43/kWh [58]. All feasible system types shown in both tables below have a levelized COE slightly higher than the national tariff. However, they are within the range of global tariff and much lower than what a previously studied result showed.

Table 6.1: Overall optimization results (HOMER)

PV (KW)	HY-5 turbine(KW)	Biogas Gen(KW)	Battery	Converter(kW)	Dispatch Strategy	Initial capital($)	Total NPC ($)	COE ($/kWh)	Renewable fraction	Biomass(t)	Biogas(hrs)
5	5	30	20	20	LF	90,610	170,140	0.268	1	422	1,450
	5	30	20	20	LF	80,610	170,757	0.269	1	495	1,701
10	5	30	20	20	LF	100,610	173,474	0.273	1	376	1,299
20		30	20	20	LF	95,660	176,408	0.277	1	470	1,578
5	5	30	20	30	LF	97,610	177,068	0.278	1	411	1,412
5	5	30	30	20	LF	98,940	177,515	0.279	1	388	1,340
	5	30	30	20	LF	88,940	178,098	0.280	1	461	1,586
	5	30	20	30	LF	87,610	178,506	0.281	1	490	1,680
10		30	20	20	LF	75,660	178,835	0.281	1	624	2,097
10		40	20	20	LF	80,660	178,980	0.281	1	599	1,564
10	5	30	20	30	LF	107,610	179,119	0.282	1	356	1,230
20		30	30	20	LF	103,610	179,383	0.282	1	406	1,395
5	5	30	30	30	LF	105,940	181,419	0.285	1	357	1,221
10	5	30	30	30	LF	115,940	182,158	0.286	1	293	1,007
10	5	30	30	20	LF	108,940	182,744	0.287	1	355	1,271
5	5	40	20	20	LF	95,610	183,397	0.288	1	487	1,271
	5	40	20	20	LF	85,610	183,558	0.289	1	557	1,454

Looking at some of the set up listed above on the overall form, we find the following remarkable results. The most cost effective system, i.e. the system with the lowest net present cost, is the PV-wind-biogas-battery-converter setup with the biogas generator operates under a load flowing (LF) strategy (whereby the biogas generator operates to produce just enough power to meet the primary load; lower-priority objectives, such as charging the battery bank or serving the deferrable load, is left to the other renewable power sources, i.e. wind and solar). For this set-up, the total net present cost (NPC) is $170,140, the cost of energy (COE) is 0.268 $/kWh, the amount of biogas (cattle's manure) used annually is 422 tonnes and the biogas generator operates for 1,450 hours per year.

In this set-up, there is an excess electricity generation of 23.8%, no unmet electric load and no capacity shortage. This could be a best choice for implementation. Figure 6.1 shows the monthly average electrical production of this system. Table 6.2 gives some of the main information about the system. The cost breakdown supported by a bar-graph for this set-up is also given in figure 6.2.

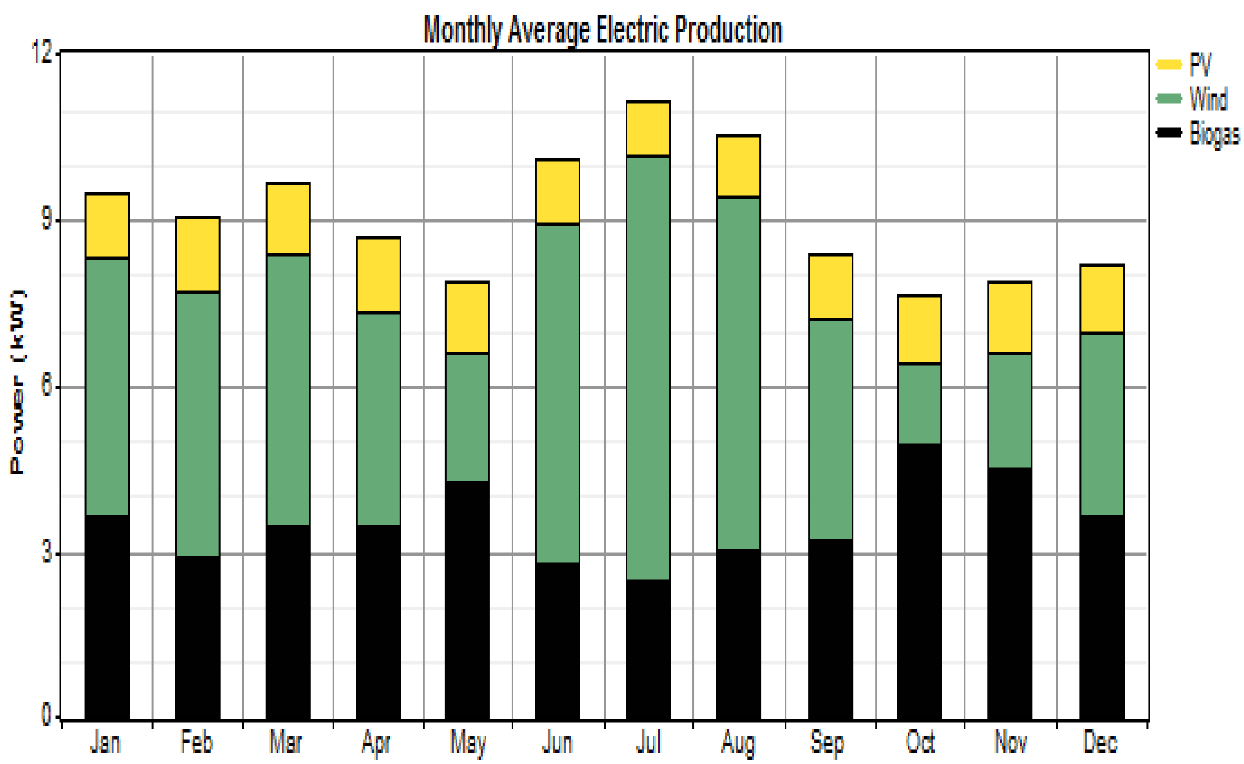

Figure 6.1: Contribution of the power units for the most cost effective system, 1st row Table 6.1

Table 6.2: System report for the most cost effective system, 1st row in Table 6.1

System architecture	
PV	5KW
Wind turbine	5
Biogas	30KW
Battery S6CS25P	20
Converter	20KW

Sensitivity case	
Solar data	6.28 KWh/m^2/day
Wind data	4.42 m/s
Cattle manure	104 tonnes/day
PV Capital Cost Multiplier	1
PV Replacement Cost Multiplier	1

Annual electric energy production (KWh/year)		
PV	10,619	13%
Wind turbine	37,808	48%
Biogas generator	30,815	39%
Excess electricity	18,836	23.8%
Unmet load		0
Capacity shortage		0

Annual electric energy consumption (KWh/year)		
Primary load	51,465	93%
Deferrable load	3,971	7%
Total	55,436	100 %
Cost summary		
NPC	$170,140	
COE	0.268 $/KWh	

Emission (kg/year)	
CO2	73
CO	2.74
Unburned hydrocarbons	0.304
Particulate matter	0.207
SO2	0
NOx	24.5

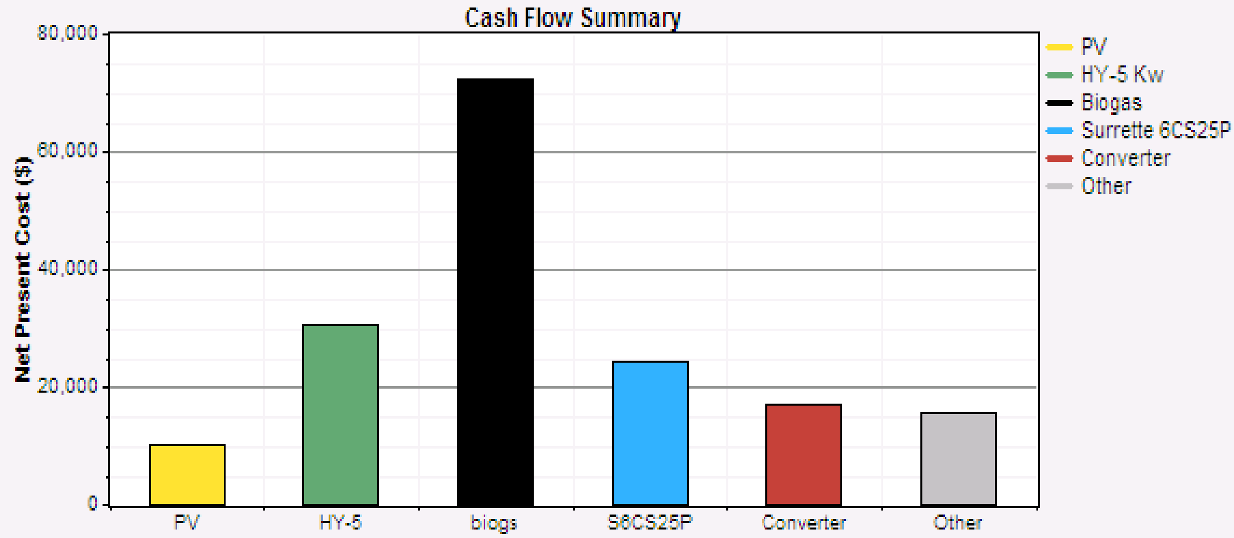

Component	Capital ($)	Replacement ($)	O&M ($)	Fuel ($)	Salvage ($)	Total ($)
PV	10,000	0	0	0	0	10,000
HY-5 Kw	24,950	0	5,735	0	0	30,685
Biogas	15,000	0	299	58,055	-1,029	72,325
Surrette 6CS25P	16,660	5,516	3,441	0	-1,154	24,464
Converter	14,000	5,842	0	0	-2,910	16,932
Other	10,000	0	5,735	0	0	15,735
System	90,610	11,358	15,210	58,055	-5,093	170,140

Figure 6.2: Cost summary for the most cost effective system, 1st row in Table 6.1

The second most cost effective system, row 2 in Table 6.1, is another system with the generator operating under Load following (LF) strategy. The NPC for this setup is $170,757 and the COE is 0.269$/kWh. The cattle's manure (biogas) used annually is 495 tonnes and the corresponding generator operation time is 1,701 hours per year. There is no PV in this system. However, it has excess electricity generation of 17.5%, no unmet electric load and no capacity shortage and this set up can be a good choice also to implement. Figure 6.3 shows the monthly average electrical system is also given in Table 6.3. The cost breakdown supported by a column-chart is also given in Figure 6.4.

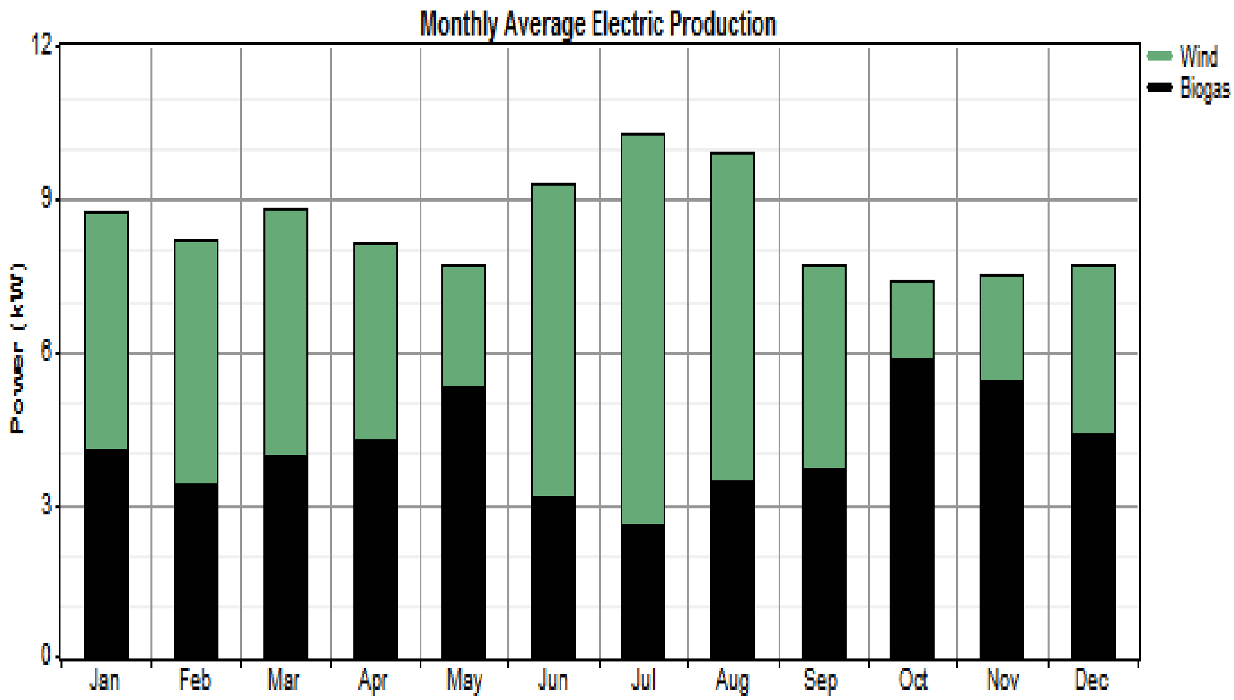

Figure 6.3: Contribution of the power units for the second most cost effective system, 2nd row in Table 6.1

Table 6.3: System report for the second cost effective system, 2nd row in Table 6.1

System architecture	
PV	
Wind turbine	5
Biogas	30KW
Battery S6CS25P	20
Converter	20KW

Sensitivity case	
Solar data	6.28 $KWh/m^2/day$
Wind data	4.42 m/s
Cattle manure	104 tonnes/day
PV Capital Cost Multiplier	1
PV Replacement Cost Multiplier	1

Annual electric energy production (KWh/year)		
PV	0	0
Wind turbine	37,808	51%
Biogas generator	36,173	49%
Excess electricity	12,966	17.5%
Unmet load		0
Capacity shortage		0

Annual electric energy consumption (KWh/year)		
Primary load	51,465	93%
Deferrable load	3,974	7%
Total	55,439	100%
Cost summary		
NPC	$170,757	
COE	0.269 $/KWh	

Emission (kg/year)	
CO2	85.7
CO	3.22
Unburned hydrocarbons	0.356
Particulate matter	0.243
SO2	0
NOx	28.7

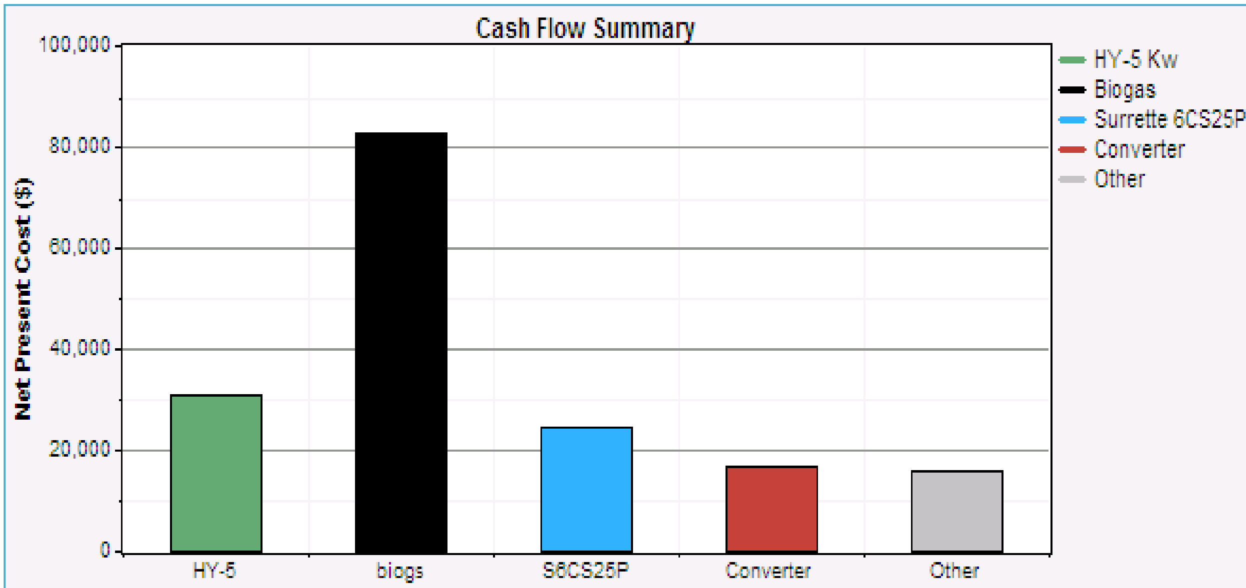

Component	Capital ($)	Replacement ($)	O&M ($)	Fuel ($)	Salvage ($)	Total ($)
HY-5 Kw	24,950	0	5,735	0	0	30,685
Biogas	15,000	0	351	68,150	-559	82,942
Surrette 6CS25P	16,660	5,516	3,441	0	-1,154	24,464
Converter	14,000	5,842	0	0	-2,910	16,932
Other	10,000	0	5,735	0	0	15,735
System	80,610	11,358	15,262	68,150	-4,623	170,757

Figure 6.4: Cost summary for the second most cost effective system, 2nd row in Table 6.1

Down in the list, the third most cost effective system, row 3 in Table 6.1, is the same system type with that of first row. For this set-up the total net present cost (NPC) is $173,474, the cost of energy (COE) is 0.273$/kWh, annual cattle manure usage is 376 tonnes and the biogas generator operates for 1,299 hours in the year. This system has excess electricity generation of 30.6%, no unmet electric load and no capacity shortage. The monthly average electric production for this setup is shown in Figure 6.5 and Table 6.4 gives the most import information about the system. The cost breakdown supported by a bar-graph for this set-up is also given in Figure 6.6.

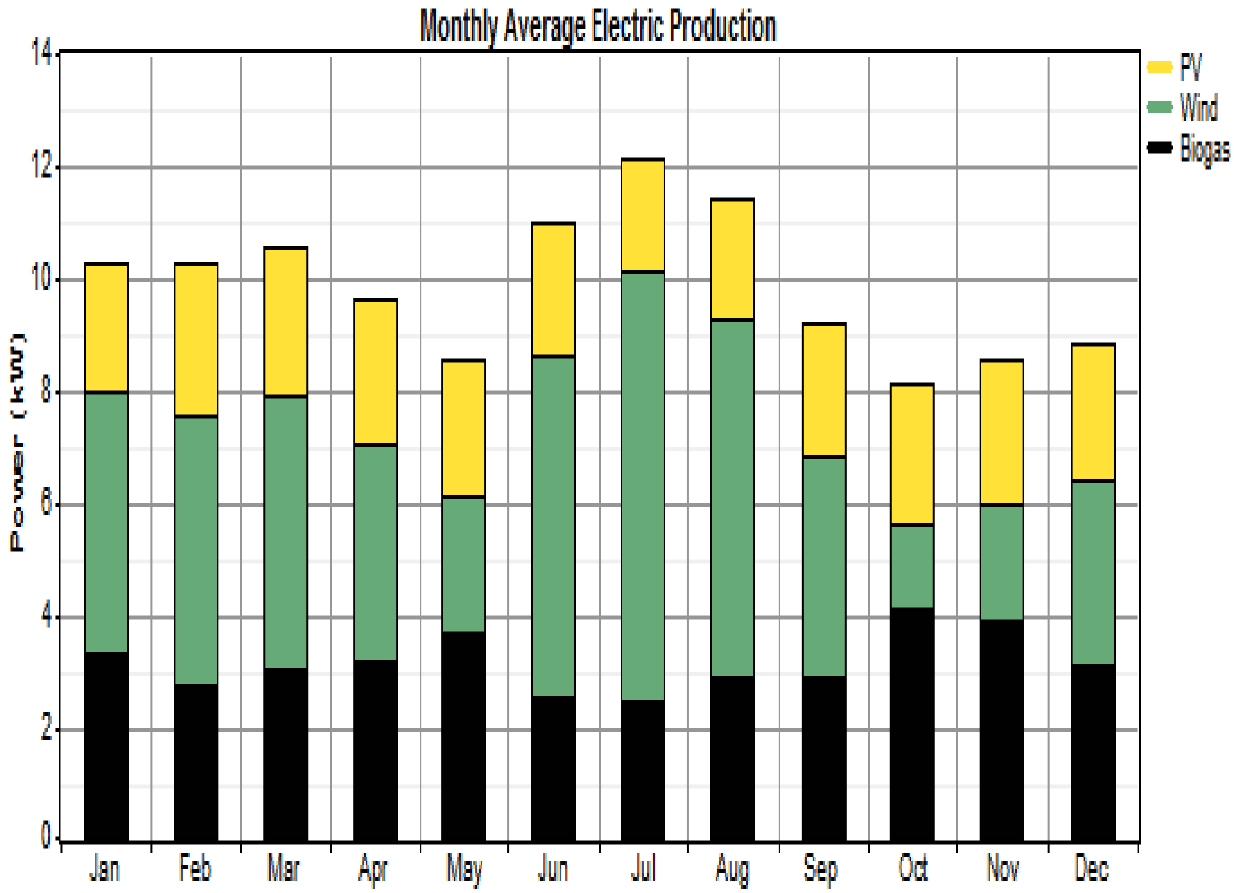

Figure 6.5: Contribution of the power units for the third cost effective system, 3rd row in Table 6.1

Table 6.4: System report for the third cost effective system, 3rd row in Table 6.1

System architecture	
PV	10KW
Wind turbine	5
Biogas	30KW
Battery S6CS2P	20
Converter	20KW

Sensitivity case	
Solar data	6.28 KWh/m^2/day
Wind data	4.42 m/s
Cattle manure	104 tonnes/day
PV Capital Cost Multiplier	1
PV Replacement Cost Multiplier	1

Annual electric energy production (KWh/year)		
PV	21,238	25%
Wind turbine	37,808	44%
Biogas generator	27,442	32%
Excess electricity	26,498	30.6%
Unmet load		0
Capacity shortage		0

Annual electric energy consumption (KWh/year)		
Primary load	51,465	93%
Deferrable load	3,971	7%
Total	55,436	100%

Cost summary	
NPC	$173,474
COE	0.273 $/KWh

Emission (kg/year)	
CO2	65
CO	2.44
Unburned hydrocarbons	0.27
Particulate matter	0.108
SO2	0
NOx	21.8

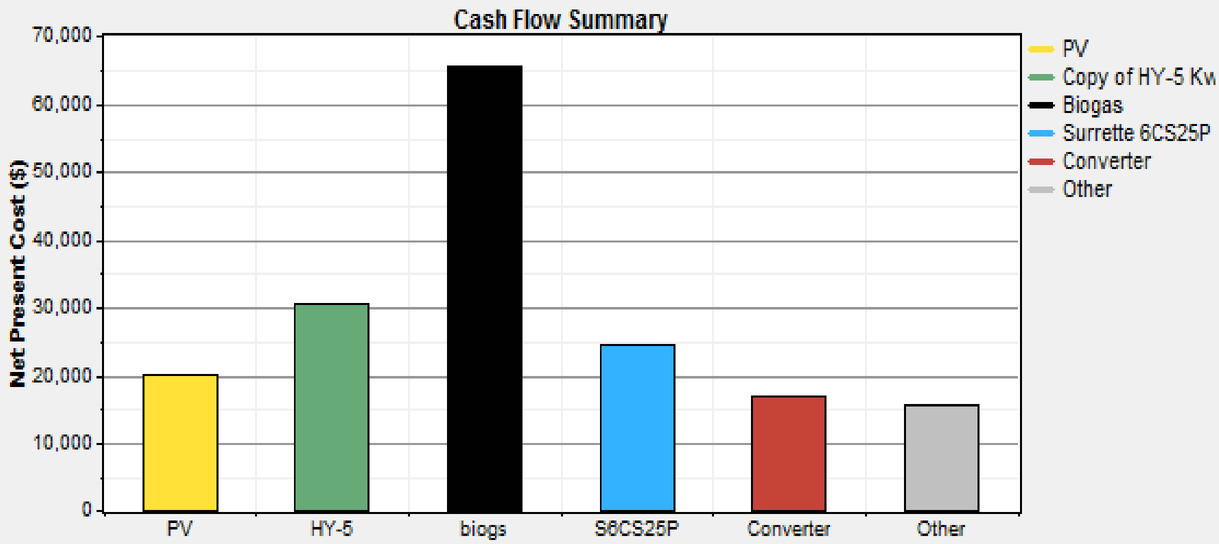

Component	Capital ($)	Replacement ($)	O&M ($)	Fuel ($)	Salvage ($)	Total ($)
PV	20,000	0	0	0	0	20,000
Copy of HY-5 Kw	24,950	0	5,735	0	0	30,685
Biogas	15,000	0	268	51,702	-1,311	65,659
Surrette 6CS25P	16,660	5,516	3,441	0	-1,154	24,464
Converter	14,000	5,842	0	0	-2,910	16,932
Other	10,000	0	5,735	0	0	15,735
System	100,610	11,358	15,179	51,702	-5,375	173,474

Figure 6.6: Cost summary for the third cost effective system, 3rd row in Table 6.1

The result in a categorized form, where only the least cost effective system is considered for each system type, is given in Table 6.5. The setup in the first row and second row of this Table is the same as that listed in Table 6.1 of first row and third row respectively, and has been discussed earlier. In this table two system set-ups are of greatest interest, each supplying 100% from renewable resources. The first one comprises PV, Biogas generator, Battery, and Converter and the second one consists of Biogas generator, Battery and Converter. The NPC for the first is $176,408 and that for the second is $197,125. The COE are 0.277$/kWh and 0.310$/kWh respectively.

Table 6.5: Results of the simulation in categorized form (HOMER)

PV (KW)	HY-5 turbine(KW)	Biogas(KW)	Battery	Converter(kW)	Dispatch Strategy	Initial Capital($)	Total NPC ($)	COE ($/kWh)	Renewable Fraction	Biomass(t)	Biogas(hrs)
5	5	30	20	20	LF	90,610	170,140	0.268	1	422	1,450
	5	30	20	20	LF	80,610	170,757	0.269	1	495	1,701
20		30	20	20	LF	95,660	176,408	0.277	1	470	1,578
		30	20	20	LF	55,660	197,125	0.310	1	878	2,958
30	5		90	30	CC	190,920	241,920	0.383	1		
50			90	40	CC	212,970	259,685	0.412	1		
	5	30			LF	49,950	267,575	0.421	1	1,419	4,837
5	5	30		20	LF	73,950	269,352	0.424	1	1,253	4,258
10		30		20	LF	59,000	324,614	0.511	1	1,760	5,928
		30			LF	25,000	356,360	0.560	1	2,216	7,512
	30		200	30	CC	347,300	469,879	0.744	1		

Sensitivity analysis was also carried out and Figure 6.7 below shows the variation of PV capital cost multiplier against wind speed variation for a fixed average solar radiation of 6.28 kWh/m^2/day and average cattle's manure (biogas resource) of 104 tonnes/day. In the Figure, the net present cost of the most cost-effective set-up for a particular set of wind speed and PV prices is also included. At lower wind speed (<4.1m/s), PV/biogas/battery system is cost effective and insensitive to wind speed variation. When the wind speed is slightly increased (4.1 to 4.6m/s), PV/biogas/battery and wind/PV/biogas/battery system are more cost effective at lower and higher PV module prices, respectively. When the wind speed is increased more (>4.6 m/s) while, PV/biogas/battery, wind/PV/biogas/battery and wind/biogas/battery systems become more favoured with lower, medium and higher PV modules prices, respectively.

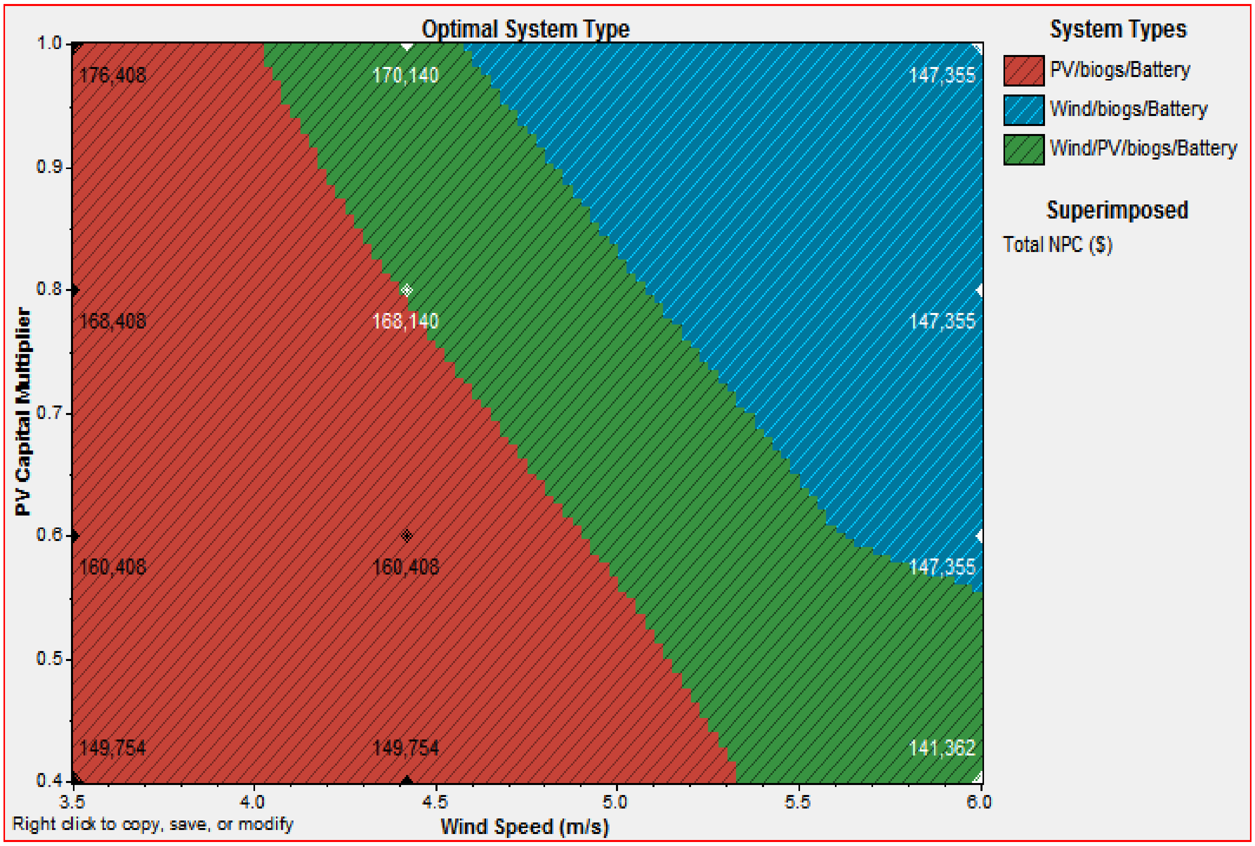

Figure 6.7: Sensitivity of PV cost to wind speed with some important NPCs labeled

HOMER software is also used to compare the investment cost of the hybrid system against the cost required for extending the grid. As a result, it is found that the hybrid system is cost effective for an area which is found at a distance greater than 14.9km (which is the breakeven grid extension distance) from the existing grid found nearby.

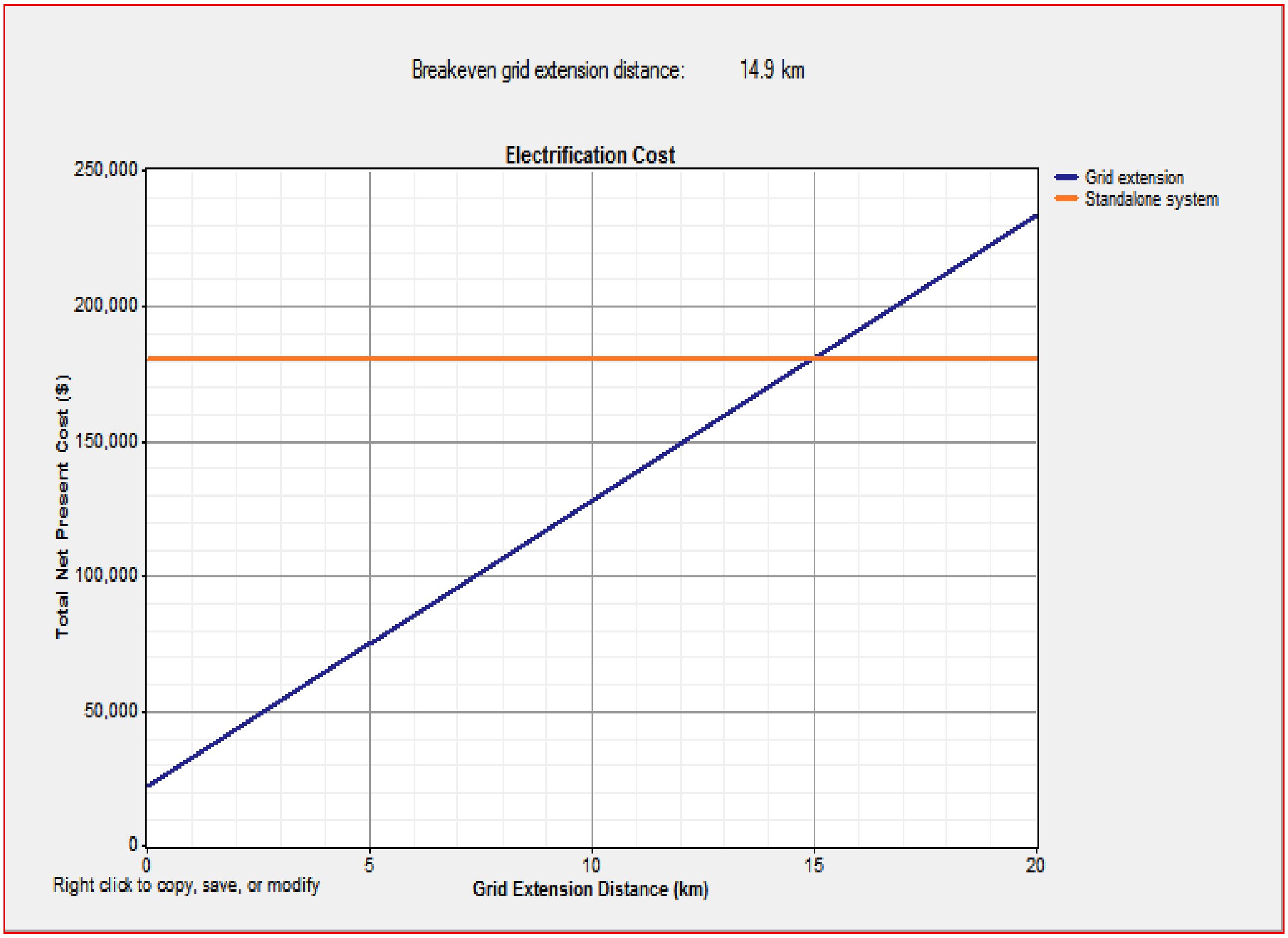

Figure 6.8: Breakeven grid extension distance obtained using HOMER

6.2. Conclusions

In this thesis, feasibility study of PV/wind/biogas hybrid energy system for electrification of 200 household in Adigrat district is done. It also compares cost of the hybrid system against the cost required to electrify the village by extending the grid. Biogas resources, wind resource, solar potentials in the district are analyzed. Finally, HOMER is used for optimization, sensitivity analysis of the proposed hybrid system.

Solar radiation is calculated from daily sunshine hour data using empirical formulas taken from NMSA of Ethiopia and is 6.28kWh/m^2/day. This result is compared with the data collected from NASA and SWERA and it is found to be nearly the same. Consequently, for this study the calculated solar radiation is used for modeling the hybrid system. Monthly average wind speed data from NASA is used to synthesize hourly wind speed data using HOMER and the data required for biogas which is the cattle's manure is collected from Ethiopian Ministry of Mines and Energy (MME). The data needed for calculating the cost of extending the grid is taken from EEPCo, and this is analyzed using interlinked Microsoft office excel spread sheet prepared by UEAP.

Hourly electric load of the community consisting of lighting, TV set, radio receiver, health post, school, water pumps and flour mills is determined. The total community is estimated to have a primary peak demand of 30 kW, a deferrable peak demand of 2.2 kW and a storage capacity of 35.64 kWh.

For the community, different feasible system configurations with different level of total NPC are obtained. The levelized COE ranges from \$0.268/kWh to \$0.289/kWh. This cost is higher than the current energy tariff within the country (< \$0.04/kWh), but, it is much less than the previously studied PV/Wind based hybrid system (which does not include biogas). It can be said that the maximum COE determined here is at the lower range of global electricity tariff.

Taking the average wind speed of 4.42 m/s and a PV capital and replacement cost of \$2000/kW, different system configurations/types are found as feasible options for the site. One feasible system from the site can be taken to make-up the overall system capable of supplying the whole community (200 household). For the overall system, PV/biogas/battery are more cost economical at lower PV module price and are not sensitive to wind speed variation. When wind speed increases slightly from 4.1 to 4.6m/s, PV/biogas/battery and PV/wind/biogas/battery systems become more favoured at lower and higher PV module price, respectively. When the wind speed is increased more (>4.6m/s), while PV/biogas/battery, PV/wind/biogas/battery and wind/biogas/battery systems become more favoured with lower, medium, higher PV module prices, respectively.

One sample overall system containing the PV-wind-biogas-battery-converter setup shows a COE of \$0.268/kWh and a total net present cost (NPC) of \$170,140. This system has excess electricity generation of 23.8%, no capacity shortage and no unmet electric load. Although the proposed system has a relatively higher COE than the national tariff, in view of the energy shortage at the national level, resistance to deforestation, clean energy development, changing the life of the poor society in remote regions and expansion of power generation, it is a highly recommendable solution.

Finally, HOMER software is also used to compare the investment cost of the hybrid system against the cost required for extending the grid. As a result, it is found that the hybrid system is cost effective for an area which is found at a distance greater than 14.9 km (which is the breakeven grid extension distance) from the existing grid found nearby.

6.3. Recommendations

- The study only focused on one selected village of Tigray region in Ethiopia and it doesn’t cover all villages around Tigray region. So, the future researchers should expand this research work in other sites of the region and make the rural people beneficiary with renewable energy resource.
- In spite of Ethiopia's huge hydropower potential, severe power outages in recent years have been recorded. Solar thermal technology, Wind power and biogas energy is recommended to be incorporated for the future grid connected application to create a strength, reliability and maintaining sustainable energy supply of the country. This site has a great solar, wind and biogas resource potential but the resources have not been exploited properly yet.
- As far as environmental issues are concerned, these kinds of hybrid systems have to be wide spread in order to reduce greenhouse effects and pollution of the environment.

References

[1] Dawit Diriba Guta,2012 "Assessment of Biomass Fuel Resource Potential And Utilization in Ethiopia: Sourcing Strategies for Renewable Energies" Vol.2, No.1, 2012 Management', Guest editorial, Information Systems Frontiers, vol. 2, no. 3-4, pp. 251- 252.

[2] Hadagu A., 2006 "Status and trends of Ethiopian rural Electrification Fund", http://www.bgr.de/geotherm/ArGeoC1/pdf/07%20A.%20Hadgu%20status%20of%20Ethiopian%20Electrification%20fund.pdf

[3] Dalelo A., 2003 "Rural Electrification in Ethiopia Opportunities and Bottlenecks", Addis Ababa University: http://www.zef.de/fileadmin/webfiles/renewables/praesentations/Dalelo_rural%20electrification%20ethiopia.pdf

[4] Drake F. and, Mulugetta Y., 1996, "Assessment of solar and wind energy in Ethiopia. I. Solar energy", *Solar Energy,* Vol. 57, No. 3, pp. 205-217, 1996

[5] Mulugetta Y. and Drake F., 1996, "Assessment of solar and wind energy resources in Ethiopia: II. Wind energy", *Solar Energy,* Vol. 57, No. 4, pp. 323-334

[6] Bekele G. and Palm B, 2010, "Feasibility Study for a Standalone Solar-Wind Hybrid Energy System for Application in Ethiopia", *Applied Energy,* Vol. 87, Issue 2, pp. 487–495.

[7] Bekele G. and Palm B.,2009 "Wind energy potential assessment at four typical locations in Ethiopia", *Applied Energy,* Vol. 86, Issue 3, pp. 388–396

[8] Tamrat B, 2007 "Comparative Analysis of Feasibility of Solar PV, Wind and Micro Hydropower Generation for Rural Electrification in the Selected Sites of Ethiopia", Addis Ababa University MSc. Thesis, July 2007

[9] Janani Chakravarthi."Biogas and energy production from cattle waste" IEEE Energy conversion conference.

[10] J. K. Maherchandani, Chitranjan Agarwal, Mukesh Sahi. (2012). Economic feasibility of Hybrid Biomass/PV/Wind systems for remote villages using Homer. India: College of Tech.& Engg.,Udaipur

[11] Kanase-Patil A.B., Saini R.P., Sharma M.P., 2010 "Integrated Renewable Energy Systems for Off Grid Rural Electrification of Remote Area", *Renewable Energy,* Vol. 35, Issue 6, pp. 1342–1349

[12] S. Diaf 1*, D. Diaf, M. Belhamel, M. Haddadi, A. Louche,2010"A methodology for optimal sizing of autonomous hybrid PV/wind system". France: Ajaccio

[13] Danish Wind Industry Association, (Jan., 2011), http://www.windpower.org/en/tour

[14] Luque, A. and Hegedus, S., (Ed) (2003) *Handbook of Photovoltaic Science and Engineering.* West Sussex, England: John Wiley & Sons Ltd.

[15] Bizuayehu T.(2011) "Improved Sustainable Power Supply for Dagahabur and Kebridahar Town of Somalia Region in Ethiopia", Reykjavik University Master's thesis ,January 2011

[16] Patel, M.R., (2006) *Wind and Solar Power Systems: Design, Analysis, and Operation.* 2nd Ed. Boca Raton: Taylor & Francis Group.

[17] Duffie, J.A. and Beckman, W.A., (2006) *Solar Engineering of Thermal Processes*. 3rd ed. New Jersey: John Wiley and Sons, Inc.

[18] Tzanakis, I., (2006) *"Combining Wind and Solar Energy to Meet Demands in the Built Environment": (Glasgow-Heraklion Crete Analysis).* MSc Thesis, University of Strathclyde.

[19] Twidell J. And Weir T, 2006, "Renewable Energy Resources", 2nd Edn, Taylor & Francis, London, 2006

[20] Aldo V., 2005, "Fundamentals of Renewable Energy processes", Elsevier Inc., 2005

[21] Patil, Mukind R., 1999, "Wind and Solar Power Systems", CRC pres LLC, USA,1999

[22] Japanese Embassy in Ethiopia, 2008 "Study on the Energy Sector in Ethiopia":
http://www.et.emb-japan.go.jp/electric_report_english.pdf

[23] Breyer Ch., Gerlach A., Hlusiak M., Peters C., Adelmann P., Winiecki J., Schützeichel H.,Tsegaye S., Gashie W., 2009 "Electrifying the Poor: Highly Economic Off-Grid PV Systems in Ethiopia a Basis for Sustainable Development"
http://www.arcfinance.org/pdfs/news/EthiopiaPaper2009.pdf

[24] Gipe, P. (2004). Wind Power: Renewable Energy for Home, Farm, and Business.

[25] Wagner, H. and Mathur, J., (2009) Introduction to Wind Energy Systems: Basics, Technology and Operation. Berlin Heidelberg: Springer-Verlag.

[26] Rivera, M.R., (2008) *Small Wind / Photovoltaic Hybrid Renewable Energy System Optimization.* MSc. Thesis, University of Puerto Rico.

[27] Manwell J.F., McGowan, J.G., Rogers, A.L., 2002, *Wind Energy Explained, Theory, Design and Application*, Wiley, UK

[28] Boyle, G. (1996). *"Renewable Energy – Power for a sustainable future".*

[29] Masters, G. M. (2004.). . *Renewable and Efficient Electric Power Systems, page 310. John Wiley & Sons, Incorporated. Hoboken,.* NJ, USA, .

[30] Bekele G., 2009, “The Study Into the Potential and Feasibility of Standalone Solar- Wind Hybrid Electric Energy Supply System for Application in Ethiopia”, KTH Royal Institute of Technology Doctoral Thesis, December 2009

[31] National Non-Food Crops Centre. "NNFCC Renewable Fuels and Energy Factsheet: Anaerobic Digestion", Retrieved on 2013-02-16

[32] Biogas & Engines, www.clarke-energy.com, Accessed 21.4.13

[33] "Biomethane fueled vehicles the carbon neutral option" Claverton Energy Conference, 24 October 2009, Bath, UK

[34] Fachagentur Nachwachsende Rohstoffe e.V. (FNR) (2009): Biogas Basis daten Deutschland – Stand: Oktober 2008. 7p. Very short but comprehensive overview of the biogas situation in Germany.
http://www.fnr-server.de/ftp/pdf/literatur/pdf_185-basisdaten_biogas_2009.pdf]

[35] National Biogas Program Ethiopia, introduction to biogas technology-user’s manual, November 2010.

[36] Madigan, T.M., Martinko, J.M. and Parker J. (2003). Brock Biology of Microorganisms (10^{th} ed). Pearson Education, Inc., Upper Saddle River, New Jersey.

[37] Al Seadi, T. (2001). Good practice in quality management of AD residues from biogas production. Report made for the International Energy Agency, Task 24- Energy from Biological Conversion of Organic Waste. Published by IEA Bioenergy and AEA Technology Environment, Oxford shire, United Kingdom.

[38] Al Seadi T., Rutz D., Prassl H., Köttner M., Finsterwalder T., Volk S. and Janssen R. (2008), "Biogas Hand Book" , Published by University of Southern Denmark Esbjerg, Niels Bohrs Vej 9-10,ISBN 978-87-992962-0-0

[39] Kanwardeep singh,(2010)"Study of Solar/Biogas Hybrid Power Generation", MSc Thesis, Thapar university ,July 2010

[40] Agapitidis I. and Zafiris C. (2006). 'Energy Exploitation of Biogas: European and National perspectives'.2nd International Conference of the Hellenic Solid Waste Management Association.

[41]Elmar Dimpl (2010)," Small-scale Electricity Generation from Biomass " Part II: Biogas 1st edition, August 2010.

[42] https://energypedia.info/wiki/Electricity-Generation-from-Biogas accessed at July10, 2013

[43] http://**www.energysolutionscenter.org**

[44] FAO (Food and Agricultural Organization of the United Nations) 2010 Global forest resources assessment, FAO Forestry paper163, 2010.

[45] HOMER, the Micropower optimization model, ver. 2.67 Beta (April, 2008), http://www.nrel.gov/homer

[46] EEPCo, UEAP. Electric Power Distribution Network Design and Construction Training Manual

[47] Nema, P., Nema, R.K., Rangnekar, S. (2010) 'PV-solar / wind hybrid energy system for GSM/CDMA type mobile telephony base station', *International Journal of Energy and Environment* 1(2), pp.359-366 (available from: www.IJEE.IEEFoundation.org)

[48] Lambert, T., Gilman, P., Lilienthal, P. (2005) 'Micro-power System modeling with Homer', in Farret, F.A., Godoy Simões, M. (eds), *Integration of alternative sources of energy,* pp. 379 - 417

[49] Solar Buzz Web Site: http://www.solarbuzz.com/solarindex/expo.asp /

[50] Solar Panel Price: http://www.solarpanelprices.org/

[51] HUAYING Wind Turbine: http://www.huayingwindpower.com/

[52] All Small Wind Turbines website: http://www.allsmallwindturbines.com/

[53] Biogas generator price: http://www.cncamda.en.alibaba.com accessed 18 May 2013

[54] Cummins Biogas Generator Data Sheet: http://www.rieanpishroco.com/cummins/

[55] Munuswamy, S., Nakamura, K., Katta, A. (2011) 'Comparing the cost of electricity sourced from a fuel cell-based renewable energy system and the national grid to electrify a rural health centre in India: A case study', *Renewable Energy* 36, pp. 2978 - 2983

[56] Deshmukh, M.K., Deshmukh, S.S. (2008) 'Modeling of hybrid renewable energy systems', *Renewable and Sustainable Energy Reviews* 12, pp. 235–249.

[57] Givler, T., Lilienthal, P., (2005) 'Using HOMER® Software, NREL's Micropower Optimization Model, To Explore the Role of Gen-sets in Small Solar Power Systems Case Study: Sri Lanka', Technical Report NREL/TP-710-36774, available from http://www.osti.gov/bridge

[58] Global Electricity Price: http://en.wikipedia.org/wiki/Electricity_tariff

Appendix A: Overall Optimization Results Table

Table A-1: Overall optimization results

PV (KW)	HY-5 turbine	Biogas Gen	Battery	Converter(kW)	Dispatch Strategy	Initial capital	Total NPC ($)	COE ($/kWh)	Renewable fraction	Biomass(t)	Biogas(hrs)
5	5	30	20	20	LF	90,610	170,140	0.268	1	422	1,450
	5	30	20	20	LF	80,610	170,757	0.269	1	495	1,701
10	5	30	20	20	LF	100,610	173,474	0.273	1	376	1,299
20		30	20	20	LF	95,660	176,408	0.277	1	470	1,578
5	5	30	20	30	LF	97,610	177,068	0.278	1	411	1,412
5	5	30	30	20	LF	98,940	177,515	0.279	1	388	1,340
	5	30	30	20	LF	88,940	178,098	0.280	1	461	1,586
	5	30	20	30	LF	87,610	178,506	0.281	1	490	1,680
10		30	20	20	LF	75,660	178,835	0.281	1	624	2,097
10		40	20	20	LF	80,660	178,980	0.281	1	599	1,564
10	5	30	20	30	LF	107,610	179,119	0.282	1	356	1,230
20		30	30	20	LF	103,990	179,383	0.282	1	406	1,395
5	5	30	30	30	LF	105,940	181,419	0.285	1	357	1,221
10	5	30	30	30	LF	115,940	182,158	0.286	1	293	1,007
10	5	30	30	20	LF	108,940	182,744	0.287	1	355	1,230
5	5	40	20	20	LF	95,610	183,397	0.288	1	487	1,271
	5	40	20	20	LF	85,610	183,558	0.289	1	557	1,454
10	5	30	20	20	CC	100,610	184,077	0.289	1	453	1,269
10		30	30	20	LF	83,990	184,555	0.290	1	580	1,946
	5	30	30	30	LF	95,940	184,751	0.291	1	449	1,535
20		30	20	30	LF	102,660	184,793	0.291	1	470	1,575
	10	30	20	20	LF	105,560	184,846	0.291	1	380	1,312
20		30	20	20	CC	95,660	185,004	0.291	1	536	1,376
20		40	20	20	LF	100,660	185,322	0.291	1	505	1,318

5	5	30	20	40	LF	104,610	185,534	0.292	1	411	1,412
30		30	20	20	CC	115,660	185,754	0.292	1	396	1,366
5	5	40	20	30	LF	102,610	186,144	0.293	1	448	1,168
5	5	30	20	20	LF	90,610	186,694	0.294	1	540	1,602
10		40	30	20	LF	88,990	186,826	0.294	1	569	1,485
	5	30	20	40	LF	94,610	186,972	0.294	1	490	1,680
5		30	20	20	LF	65,660	187,136	0.294	1	745	2,511
10		30	20	20	LF	82,660	187,301	0.295	1	624	2,097
10	5	30	20	40	LF	114,610	187,584	0.295	1	356	1,230
20		30	30	30	LF	110,990	187,933	0.296	1	407	1,383
10	5	40	20	30	LF	112,610	188,093	0.296	1	392	1,023
10		40	20	30	LF	87,660	188,168	0.296	1	604	1,577
5	10	30	20	20	LF	115,560	188,497	0.296	1	337	1,162
5	5	40	30	30	LF	110,940	189,270	0.298	1	385	1,004
10	5	40	30	30	LF	120,940	189,387	0.298	1	317	826
20		40	20	30	LF	107,660	189,401	0.298	1	475	1,239
	5	40	20	30	LF	92,610	189,525	0.298	1	540	1,409